

**USC-SIPI REPORT #195**

**Cumulant-Based Blind Optimum  
Beamforming**

**by**

**Mithat C. Dogan and Jerry M. Mendel**

**January 1992**

**Signal and Image Processing Institute  
UNIVERSITY OF SOUTHERN CALIFORNIA  
Department of Electrical Engineering-Systems  
3740 McClintock Avenue, Room 404  
Los Angeles, CA 90089-2564 U.S.A.**

## Abstract

Sensor response, location uncertainty and use of sample statistics can severely degrade the performance of optimum beamformers. In this report, we propose blind estimation of the source steering vector in the presence of multiple, directional, correlated or coherent Gaussian interferers via higher-order-statistics. In this way, we employ the statistical characteristics of the desired signal to make the necessary discrimination, without any a-priori knowledge of array manifold and direction-of-arrival information about the desired signal. We then improve our method to utilize the data in a more efficient manner. In any application, only sample statistics are available, so we propose a robust beamforming approach that employs the steering vector estimate obtained by cumulant-based signal processing. We further propose a method that employs both covariance and cumulant information to combat finite sample effects. We analyze the effects of multipath propagation on the reception of the desired signal. We show that even in the presence of coherence, cumulant-based beamformer still behaves as *the* optimum beamformer that maximizes the Signal to Interference plus Noise Ratio (SINR). Finally, we propose an adaptive version of our algorithm. Simulations demonstrate the excellent performance of our approach in a wide variety of situations.

# Contents

<b>1</b>	<b>Introduction</b>	<b>1</b>
<b>2</b>	<b>Problem Formulation</b>	<b>4</b>
2.1	Signal Model . . . . .	4
2.2	Covariance-Based Approaches . . . . .	6
<b>3</b>	<b>Cumulant-Based Optimum Beamforming</b>	<b>10</b>
3.1	Higher-Order Statistics: Definitions and Properties . . . . .	11
3.2	Estimation of desired signal steering vector . . . . .	14
3.3	Interference Rejection . . . . .	15
<b>4</b>	<b>Robust Beamforming</b>	<b>17</b>
4.1	Efficient Utilization of Array Data . . . . .	17
4.2	Covariance-Cumulant ( $C^2$ ) Approach . . . . .	18
4.3	Robustness Constraint . . . . .	20
<b>5</b>	<b>Multipath Phenomena</b>	<b>23</b>
<b>6</b>	<b>Adaptive Processing</b>	<b>28</b>

<i>CONTENTS</i>	iii
<b>7 Simulations</b>	<b>31</b>
7.1 Experiment 1: Desired Signal in White-Noise . . . . .	32
7.2 Experiment 2: Spatially Colored Noise and Multipath Propagation . . . . .	36
7.3 Experiment 3: Effects of Robustness Constraint . . . . .	38
7.4 Experiment 4: Multiple Interferers . . . . .	40
7.5 Experiment 5: Adaptive Processing . . . . .	42
7.6 Experiment 6: Effects of Data Length . . . . .	43
<b>8 Conclusions</b>	<b>47</b>
<b>Appendix</b>	<b>48</b>
<b>A Third-order statistics based estimation</b>	<b>48</b>
<b>B Full utilization of array data</b>	<b>50</b>

# List of Figures

7.1	Beampatterns and white-noise gains of processors for SNR=20 dB . . . . .	33
7.2	Beampatterns and white-noise gains of processors for SNR=0 dB . . . . .	35
7.3	Power of cumulant-based beamforming . . . . .	36
7.4	Beamforming in the presence of spatially colored noise . . . . .	37
7.5	Beampattern of CUM <sub>1</sub> processor for varying virtual SNR . . . . .	39
7.6	Beampatterns and array gains of processors . . . . .	42
7.7	Beampattern of the <i>adaptive</i> CUM <sub>1</sub> processor as a function of time . . . . .	44
7.8	Performance of processors with varying data length . . . . .	46

# List of Tables

7.1	Results from 100 Monte-Carlo Runs for Experiment 1 . . . . .	34
7.2	Results from 100 Monte-Carlo Runs for Experiment 2 . . . . .	38
7.3	Signal structure for Experiment 4 . . . . .	40
7.4	Results from 100 Monte-Carlo Runs for Experiment 4 . . . . .	41

# Chapter 1

## Introduction

Array processing techniques play an important role in enhancement of signals in the presence of interference. A number of books, and an extensive literature [1]–[9] have already been published. Capon's minimum-variance distortionless response (MVDR) beamformer [10] has been a starting point for both signal enhancement and high-resolution direction-of-arrival (DOA) estimation.

In recent years, there has been an increasing interest in high-resolution array processing techniques based on eigendecomposition of the covariance matrix of received signals [11]–[21]. To recover the signal of interest in the presence of interfering signals, the so-called COPY function [17] is used. In this procedure, DOA's for all signals are first estimated, and then the minimum-variance processor that reconstructs the desired signal and minimizes the contribution of all interference sources is implemented. All of the previously referenced methods rely on complete knowledge of responses and locations of array elements and/or DOA information of the desired signal.

If the array manifold is unknown, or there are uncertainties, it is then necessary to calibrate the array [22]–[23]; however, this is not a practical thing to do, since calibration must be done quite frequently, and, each time, array-manifold information must be stored. In addition, calibration

sources may be required. Even small errors in the calibration procedure may considerably degrade the performance. Sensitivity analyses of high-resolution methods and MVDR beamforming have been presented in [24]–[32].

In this report, we shall employ higher-order statistics of received signals to estimate the steering vector of the non-Gaussian desired signal in the presence of directional Gaussian interferers with unknown covariance structure. We assume no knowledge of array manifold and DOA information about the desired signal. Desired signal may be voiced speech, sonar signal, radar return or a communication signal. In our work, we specialize to the communications scenario, which requires the use of fourth-order cumulants. Following a mathematical formulation of the problem in Chapter 2, we describe basic properties of cumulants and blind estimation and optimum beamforming procedures in Chapter 3.

Any estimation procedure is subject to errors, as is our cumulant-based source steering vector estimation method. In theory, cumulants are blind to Gaussian noise; however, their estimates are corrupted by such noise. In order to obtain satisfactory results, longer data lengths are necessary in cumulant-based signal processing. To alleviate the effects of estimation error in the beamforming step, we propose a more efficient estimation procedure that fully utilizes the data acquired by the array. We further suggest a method of combining cumulant and covariance information to yield better estimates. Then we employ a robust beamforming method based on artificial noise injection to combat mismatch in the source steering vector. We consider the estimation error as a mismatch and successfully apply this robust approach to our problem. These methods are presented in Chapter 4.

In a communications environment, multipath propagation almost always take place. In this case, all eigendecomposition-based techniques and MVDR fail. Only in some specific array configurations



is it possible to decorrelate incoming signals and then estimate their DOA's. We analyze the behavior of our cumulant-based approach in Chapter 5. We show that our proposed approach behaves as *the* optimum beamformer that maximizes the Signal to Interference plus Noise Ratio (SINR).

For real-time operation (a necessary requirement in communications applications) we propose an adaptive implementation of the cumulant-based beamformer in Chapter 6. We then present simulation experiments to indicate the performance of our approach in Chapter 7. Finally, we draw our conclusions in Chapter 8.

## Chapter 2

# Problem Formulation

We formulate our problem in a narrowband fashion. In array processing, a problem is classified as narrowband if the signal bandwidth is small compared to the reciprocal of the time required for the signal wavefront to propagate across the array. For a discussion on bandwidth, see [36]-[37].

In our formulation, lower and upper case italic letters are used to represent scalars, lower case bold-faced letters are used for vectors, and, upper case bold-faced letters are used for matrices.

### 2.1 Signal Model

Consider an array of  $M$  elements, with arbitrary sensor response characteristics and locations. Assume there are  $J$  Gaussian interference signals  $\{ i_j(t), j = 1, 2, \dots, J \}$ , and a non-Gaussian desired signal  $d(t)$ , centered at frequency  $w_o$ . We assume sources are far away from the array so that a planar wavefront approximation is possible. The additive noise present is assumed to be Gaussian with unknown covariance. With these assumptions, the received signal at the  $k$ th sensor can be expressed, as

$$r_k(t) = a_k(\theta_d) d(t) + \sum_{j=1}^J a_k(\theta_{i_j}) i_j(t) + n_k(t) \quad (2.1)$$

where,

- $\theta_x$  : the direction-of-arrival of the wavefront corresponding to emitter  $x$ .
- $a_k(\theta_x)$  : response of the  $k$ th sensor to  $x$ th signal wavefront, including the phase factor associated with the travel time of the signal wavefront with respect to a reference point; without loss of generality, this point can be taken as the first sensor location.
- $d(t)$  : the desired non-Gaussian signal as received at sensor 1, with variance  $\sigma_d^2$ .
- $i_j(t)$  : the  $j$ th interferer waveform as received at sensor 1; interference signals are assumed to be independent of the desired signal, and they are Gaussian processes.
- $n_k(t)$  : the additive noise at the  $k$ th sensor.

Equation (2.1) can be rewritten in matrix notation, as

$$\begin{bmatrix} r_1(t) \\ r_2(t) \\ \vdots \\ r_M(t) \end{bmatrix} = \begin{bmatrix} \mathbf{a}(\theta_d), \mathbf{a}(\theta_{i_1}), \dots, \mathbf{a}(\theta_{i_J}) \end{bmatrix} \begin{bmatrix} d(t) \\ i_1(t) \\ \vdots \\ i_J(t) \end{bmatrix} + \begin{bmatrix} n_1(t) \\ n_2(t) \\ \vdots \\ n_M(t) \end{bmatrix} \quad (2.2)$$

where  $\mathbf{a}(\theta_x)$  represents the  $M \times 1$  steering vector for the wavefront from emitter  $x$ , which can be expressed as

$$\mathbf{a}(\theta_x) = \begin{bmatrix} a_1(\theta_x), a_2(\theta_x), \dots, a_M(\theta_x) \end{bmatrix}^T \quad (2.3)$$

We define the *array manifold* as the collection of steering vectors over all DOA's of interest. Alternative expressions for the received signal vector are,

$$\mathbf{r}(t) = \mathbf{A} \mathbf{z}(t) + \mathbf{n}(t) = \mathbf{a}(\theta_d) d(t) + \mathbf{A}_I \mathbf{i}(t) + \mathbf{n}(t) \quad (2.4)$$

In this last expression, we partitioned the  $M \times (J + 1)$  steering matrix  $\mathbf{A}$  as,

$$\mathbf{A} = \left[ \mathbf{a}(\theta_d), \mathbf{A}_I \right] \quad (2.5)$$

where the  $M \times J$  matrix  $\mathbf{A}_I$ , is the steering matrix for interference sources.

In this report, we address the problem of optimum beamforming with an array of sensors whose responses and locations are completely unknown; hence, although we may have a priori knowledge about the direction-of-arrival of desired signal, we can not perform beamforming due to the lack of knowledge of array manifold. In [38], this problem is addressed; however, [38]'s algorithm is limited to a single interference signal. We investigate the possibility of a more general solution; namely, signal recovery in the presence of multiple interferers whose correlation structure is unknown. Before presenting our approach, which employs higher-order statistics, we demonstrate the limitations of covariance-based array processing for this problem.

## 2.2 Covariance-Based Approaches

Currently used high-resolution methods of DOA estimation and minimum-variance distortionless response beamforming (MVDR) employ the covariance matrix of signals received by the array. The wavefront covariance matrix,  $\mathbf{S}$ , is defined as the covariance of the source signals as received at the

reference point, i.e., at sensor 1:

$$\mathbf{S} = \mathcal{E} \{ \mathbf{z}(t) \mathbf{z}^H(t) \} \quad (2.6)$$

where  $(\cdot)^H$  denotes complex conjugate transpose. Using the received signal model in (2.4), we can express the  $M \times M$  covariance matrix  $\mathbf{R}$  of array measurements in the following two ways:

$$\mathbf{R} = \mathcal{E} \{ \mathbf{r}(t) \mathbf{r}^H(t) \} = \mathbf{A} \mathbf{S} \mathbf{A}^H + \mathbf{R}_n = \sigma_d^2 \mathbf{a}(\theta_d) \mathbf{a}^H(\theta_d) + \mathbf{R}_u \quad (2.7)$$

where  $\mathbf{R}_n$  is the noise covariance matrix,

$$\mathbf{R}_n = \mathcal{E} \{ \mathbf{n}(t) \mathbf{n}^H(t) \} \quad (2.8)$$

and,  $\mathbf{R}_u$  is the covariance matrix of the undesired signals, i.e.,

$$\mathbf{R}_u = \mathcal{E} \{ [ \mathbf{A}_I \mathbf{i}(t) + \mathbf{n}(t) ] [ \mathbf{A}_I \mathbf{i}(t) + \mathbf{n}(t) ]^H \} \quad (2.9)$$

In general, the noise covariance matrix,  $\mathbf{R}_n$ , is unknown. With some restrictions on array orientation and noise covariance structure, some approaches for high resolution DOA estimation are proposed in [39]-[40] that do not require this information; however, these techniques have their limitations due to involved assumptions. Even with complete knowledge of noise covariance structure, source localization is still impossible without the knowledge of array manifold. In [20], ESPRIT algorithm is devised to overcome this problem; however, ESPRIT requires transitionally equivalent subarrays with known displacement vectors, which may also be impractical due to all the constraints on array orientation. In [33], an eigendecomposition-based beamforming approach

is proposed which assumes the identifiability of the signal subspace and availability of the steering vector information for the signal of interest. Good results were obtained under these assumptions; however, this method can not handle coherent interference and spatially colored noise.

In [41]-[43], blind estimation of steering vectors for independent emitters is discussed with the following conclusion:

Blind estimation of source steering vectors is not possible with only second-order statistics, but employing higher-than-second-order cumulants, it is possible to estimate source steering vectors up to a scale factor.

MVDR beamforming is an alternate approach for signal recovery. This approach however, requires knowledge of the steering vector for the desired source up to a scale factor and uses the covariance matrix  $\mathbf{R}$  of received signals for processing. The output of the MVDR beamformer  $y(t)$  can be expressed as [10]

$$y(t) = \mathbf{w}^H \mathbf{r}(t) = [\beta_1 \mathbf{R}^{-1} \mathbf{a}(\theta_d)]^H \mathbf{r}(t) \quad (2.10)$$

where the constant  $\beta_1$  is present to maintain a specified response for the desired signal and  $\mathbf{w}$  denotes the weight vector of the processor.

From the above expression, it is clear that MVDR beamforming requires knowledge of  $\mathbf{a}(\theta_d)$ . Without knowledge of array manifold, it is not possible to determine  $\mathbf{a}(\theta_d)$  even in the case of known  $\theta_d$ . Therefore, MVDR beamforming can not be directly applied to our problem. In addition, the MVDR beamformer is quite sensitive to errors in assumed sensor locations and characteristics [24]-[29].

In many applications, multipath propagation takes place resulting in coherent sources. Coher-

ence presents a serious problem to DOA methods; it leads to a singular source covariance matrix  $\mathbf{S}$ , for which it is not possible to estimate source locations except in some specific array configurations [44]-[50]. In the MVDR case, source coherency does not represent a problem as long as there is no source correlated with the desired signal; however, this situation is rarely met in practice. In general, the desired signal is subject to multipath propagation, and performance of MVDR approach degrades severely [51]-[52]. An optimum beamforming procedure has been suggested in [53] to overcome the coherence problem by using a linear array of elements with identical directional characteristics.

We are therefore looking for a method that can overcome all these problems. In the next chapter, we present an approach that accomplishes this by combining cumulant-based blind estimation and MVDR beamforming.

## Chapter 3

# Cumulant-Based Optimum

# Beamforming

In the previous chapter, we discussed the problem of optimum beamforming and concluded that it is not possible to recover a desired signal in the presence of multiple interferers, unknown sensor noise covariance, and multipath propagation without any information about array manifold. In this chapter, we propose a method to overcome these problems. We propose a two-step procedure: higher-order-statistics for blind estimation of the source steering vector, followed by MVDR beamforming based on second-order statistics of received signals and steering vector estimate provided by the first step. Before describing our method we first present a brief review of higher-order statistics.



### 3.1 Higher-Order Statistics: Definitions and Properties

Let  $\{x_1, x_2, \dots, x_n\}$  be a collection of random variables and  $\{v_1, v_2, \dots, v_n\}$  be a collection of deterministic variables. We can stack these variables in vectors  $\mathbf{x} = [x_1, x_2, \dots, x_n]^T$  and  $\mathbf{v} = [v_1, v_2, \dots, v_n]^T$ . Then, the  $n$ th-order cumulant of the random variables is defined as the coefficient of  $(v_1, v_2, \dots, v_n)$  in the Mac-Laurin series expansion of the cumulant-generating function

$$K_{\mathbf{x}}(\mathbf{v}) = \ln ( E \{ \exp [ j \mathbf{v}^T \mathbf{x} ] \} ) \quad (3.1)$$

An alternate approach that defines the  $n$ th-order cumulant in terms of a weighted sum of joint moments of orders up to  $n$  is provided in [55].

For zero-mean real random variables, which we frequently encounter in applications, the second-, third-, and fourth-order cumulants are expressed, as

$$cum(x_1, x_2) = E \{ x_1 x_2 \}$$

$$cum(x_1, x_2, x_3) = E \{ x_1 x_2 x_3 \} \quad (3.2)$$

$$cum(x_1, x_2, x_3, x_4) = E \{ x_1 x_2 x_3 x_4 \} - E \{ x_1 x_2 \} E \{ x_3 x_4 \} -$$

$$E \{ x_1 x_3 \} E \{ x_2 x_4 \} - E \{ x_1 x_4 \} E \{ x_2 x_3 \}$$

There are several ways of collecting these random variables. In array processing, we collect samples of delayed sensor outputs; in system identification, we collect samples from a random process. In the system identification context, if  $x(t)$  is a random process, stationary up to order  $n$ , then the  $n$ th-order cumulant of  $x(t)$ ,  $C_{n,x}(\tau_1, \tau_2, \dots, \tau_{n-1})$ , is defined as the  $n$ th-order cumulant

of the random variables  $\{x(t), x(t + \tau_1), \dots, x(t + \tau_{n-1})\}$ , i.e.,

$$C_{n,x}(\tau_1, \tau_2, \dots, \tau_{n-1}) = \text{cum}(x(t), x(t + \tau_1), \dots, x(t + \tau_{n-1})) \quad (3.3)$$

Due to the stationarity assumption, the  $n$ th-order cumulant of the random process  $x(t)$  has  $(n - 1)$  degrees of freedom  $\{\tau_1, \tau_2, \dots, \tau_{n-1}\}$ . Since the  $n$ th-order cumulant can be expressed as a sum of joint moments of the random variables of orders up to  $n$ , its existence is established if all absolute moments of orders  $m \leq n$  exist and are bounded.

Note that for zero-mean processes the second- and third-order cumulants are identical to covariance and third-moment respectively. The third- and higher-order cumulants of Gaussian processes are identically zero. This fact can be used for detection and characterization of deviations from non-Gaussianity [56].

The following properties of cumulants are used frequently in applications [55]:

- [CP1] If  $\{\alpha_i\}_{i=1}^n$  are constants and  $\{x_i\}_{i=1}^n$  are random variables, then

$$\text{cum}(\alpha_1 x_1, \alpha_2 x_2, \dots, \alpha_n x_n) = \left( \prod_{i=1}^n \alpha_i \right) \text{cum}(x_1, x_2, \dots, x_n) \quad (3.4)$$

- [CP2] Cumulants are additive in their arguments.

$$\text{cum}(x_1 + y_1, x_2, \dots, x_n) = \text{cum}(x_1, x_2, \dots, x_n) + \text{cum}(y_1, x_2, \dots, x_n) \quad (3.5)$$

- [CP3] If the random variables  $\{x_i\}_{i=1}^n$  are independent of the random variables  $\{y_i\}_{i=1}^n$ , then

$$\text{cum}(x_1 + y_1, x_2 + y_2, \dots, x_n + y_n) = \text{cum}(x_1, x_2, \dots, x_n) + \text{cum}(y_1, y_2, \dots, y_n) \quad (3.6)$$

- [CP4] Cumulants suppress Gaussian noise of arbitrary covariance, i.e., if  $\{z_i\}_{i=1}^n$  are Gaussian random variables independent of  $\{x_i\}_{i=1}^n$  and  $n > 2$ , we have

$$\text{cum}(x_1 + z_1, x_2 + z_2, \dots, x_n + z_n) = \text{cum}(x_1, x_2, \dots, x_n) \quad (3.7)$$

- [CP5] If a subset of random variables  $\{x_i\}_{i=1}^n$  are independent of the rest, then

$$\text{cum}(x_1, x_2, \dots, x_n) = 0 \quad (3.8)$$

- [CP6] If  $\alpha_o$  is a constant, then

$$\text{cum}(\alpha_o + x_1, x_2, \dots, x_n) = \text{cum}(x_1, x_2, \dots, x_n) \quad (3.9)$$

Cumulants are blind to phase shifts and scale factors. This originates from their definition. Third-order cumulants are blind to processes that have a symmetric probability density function; consequently, fourth-order cumulants must be used in such environments. Cumulants of independent and identically distributed (i.i.d.) random processes are delta functions, i.e., if  $x(t)$  is such a process, then

$$C_{n,x}(\tau_1, \tau_2, \dots, \tau_{n-1}) = \gamma_{n,x} \delta_{\tau_1, \tau_2, \dots, \tau_{n-1}} \quad (3.10)$$

where  $\gamma_{n,x}$  is the  $n$ th-order cumulant of a single time sample from  $x(t)$ . It is important to note that joint moments do not possess this property. Furthermore, cumulants of order higher than two are blind to Gaussian noise and can reveal phase characteristics of the system under consideration. On the other hand, covariance-based approaches are blind to phase information and sensitive to

Gaussian noise. These properties, as proved in [57], make higher-order statistics candidates to previously unsolvable signal processing and communication problems.

In applications, we do not have access to true cumulants; we estimate them from the received data. The presence of additive Gaussian noise does effect the quality of the estimates, due to finite sample averaging in the estimation procedure. In order to get satisfactory results, longer data lengths are required for higher-order processing. An analysis of the asymptotical behavior of estimates of higher-order statistics can be found in [58].

### 3.2 Estimation of desired signal steering vector

In this section, we employ cumulants of received signals, to estimate the steering vector of the desired signal up to a constant factor. As described in Section 3.1, third-order cumulants are blind to signals with symmetric probability density function. On the other hand, most signals in communication environments have symmetric density functions, which motivates the use of fourth-order cumulants<sup>1</sup>. First, we define the *fourth-order zero-lag cumulant* operator of complex processes  $\{x_1(t), x_2(t), x_3(t), x_4(t)\}$ , based on (3.2), as

$$\begin{aligned} cum \{x_1(t), x_2(t), x_3(t), x_4(t)\} &\triangleq E \{x_1(t)x_2(t)x_3(t)x_4(t)\} - E \{x_1(t)x_2(t)\} E \{x_3(t)x_4(t)\} \\ &\quad - E \{x_1(t)x_3(t)\} E \{x_2(t)x_4(t)\} - E \{x_1(t)x_4(t)\} E \{x_2(t)x_3(t)\} \end{aligned} \quad (3.11)$$

Next, consider the vector  $\mathbf{c} = [c_1, c_2, \dots, c_M]^T$ , defined as

$$c_l \triangleq cum\{r_1(t), r_1^H(t), r_l^H(t), r_l(t)\} \quad l = 1, 2, \dots, M. \quad (3.12)$$

---

<sup>1</sup>An estimation procedure based on third-order statistics is presented in Appendix A.

As suggested in [55], there are various ways of defining fourth-order statistics of complex random processes. We follow the approach presented in [59] in (3.12). Since interference signals are independent of the desired signal and they are Gaussian with zero fourth-order cumulants ([CP4]), using (2.1) in (3.12) we can express  $c_l$  as

$$c_l = \text{cum} \{a_1(\theta_d)d(t), a_1^H(\theta_d)d^H(t), a_1^H(\theta_d)d^H(t), a_l(\theta_d)d(t)\} \quad (3.13)$$

Using [CP1], we obtain

$$c_l = |a_1(\theta_d)|^2 a_1^H(\theta_d) \gamma_{d,4} a_l(\theta_d) \quad (3.14)$$

where  $\gamma_{d,4}$  denotes the *zeroth* lag of the *fourth-order* cumulant of the desired signal. Defining  $\beta_2 = |a_1(\theta_d)|^2 a_1^H(\theta_d) \gamma_{d,4}$  we have the following expression for the  $M \times 1$  vector  $\mathbf{c}$ :

$$\mathbf{c} = \beta_2 \mathbf{a}(\theta_d) \quad (3.15)$$

Observe that the vector  $\mathbf{c}$  is a *replica of the steering vector of the desired signal up to a scale factor*.

We show in the next section how this information can be used to recover the desired signal.

### 3.3 Interference Rejection

With the knowledge of the steering vector of the desired signal, interference rejection is possible using the following minimum-variance distortionless response formulation: find the weight vector  $\mathbf{w}$  that minimizes the power,  $\mathbf{w}^H \mathbf{R} \mathbf{w}$ , at the output of the beamformer subject to the constraint  $\mathbf{w}^H \mathbf{c} = 1$ , where  $\mathbf{c}$  is obtained via the cumulant-based estimation procedure described in Sec-

tion 3.2. The solution to this optimization problem is well-known [10], and can be expressed as

$$\mathbf{w}_{cum} = \beta_3 \mathbf{R}^{-1} \mathbf{c} \quad (3.16)$$

where the constant  $\beta_3 = (\mathbf{c}^H \mathbf{R}^{-1} \mathbf{c})^{-1}$  is present in order to maintain the linear constraint.

Due to the constraint  $\mathbf{w}^H \mathbf{c} = 1$ , the power minimization procedure does not cancel the desired signal, but rejects all interference components and sensor noise in the best possible manner. Note that this is accomplished without knowledge of covariance structure of interference signals, sensor noise or array manifold. In the sequel, we refer to the processor in (3.16) as CUM<sub>1</sub>. The proof that this cumulant-based beamformer is identical to the maximum SINR processor is provided in Chapter 5, where the general multipath case is treated.

## Chapter 4

# Robust Beamforming

In this chapter, we first propose an approach that utilizes the received data in the estimation of the source steering vector in a more efficient manner. We then suggest a method that uses both cumulants and covariance information under some scenarios. Finally, we employ a robust method to combat the effects of estimation errors.

### 4.1 Efficient Utilization of Array Data

In the previous chapter, we presented a method of blind estimation of the desired source steering vector from the received data; however, the proposed approach is rather inefficient in the sense that only the first sensor is taken as reference. For example, if the connection from this element to the processor is broken, then the estimation objective can not be accomplished. Similarly, due to poor receiving circuitry following this array element, the reference signal may be very noisy, degrading the quality of the estimate. We can overcome these difficulties by using multiple reference elements.

Define the matrix  $\mathbf{C}$  with the  $(k, l)$ th element,

$$C_{k,l} \triangleq \text{cum}\{r_k(t), r_k^H(t), r_k^H(t), r_l(t)\} \quad \text{where } k, l = 1, \dots, M. \quad (4.1)$$

With true statistics, the cross-cumulant matrix  $\mathbf{C}$  will have rank 1, since all its columns are scaled replicas of the desired source steering vector; however, with sample statistics this condition never holds. The left singular vector of  $\mathbf{C}$  with the largest singular value can be used as the estimate of the desired source steering vector removing the effects of noise. In this way, we utilize array data more efficiently<sup>1</sup>. The beamformer that employs the steering vector estimate obtained in the way described above is referred to as the CUM<sub>2</sub> beamformer in the sequel.

In addition, the Total Least Squares algorithm, that takes the errors in both the received data covariance matrix estimate and the steering vector estimate into account, is a better choice for computing the optimum weight vector, as suggested in [52], but it is computationally expensive. If extra computations are feasible, we suggest the use of the Constrained Total Least Squares algorithm [60], for even better numerical results.

## 4.2 Covariance-Cumulant ( $\mathbf{C}^2$ ) Approach

In some array processing applications, sensor noise covariance structure has a definite structure enabling a whitening operation on the received data. The principal eigenvectors of the covariance matrix of this processed data reveal the subspace spanned by the steering vectors of directional signals illuminating the array [17]. Hence, the steering vector estimate obtained by the cumulant-based approach can be improved by projecting this estimate on the subspace spanned by the

---

<sup>1</sup>A method that utilizes the array data even more efficiently is presented in Appendix B.



principal eigenvectors of the covariance matrix. This improved estimate can then be used in the beamforming procedure of Section 3.3. The motivation behind this approach is that covariance estimates exhibit less variance than cumulant estimates, but in the covariance domain we can not identify the source steering vector if there are multiple sources. This procedure yields an estimate of the steering vector from covariance-matrix information by employing the cumulant-based estimate as side information. A mathematical description of this approach is presented below:

1. From the received data, estimate the covariance matrix  $\mathbf{R}$  and the desired signal steering vector  $\mathbf{c}$  by the cumulant-based procedure.
2. Perform an eigendecomposition of the sample covariance matrix, to reveal the signal and noise subspaces: the eigenvectors of  $\mathbf{R}$  with the repeated minimum eigenvalue span the noise subspace [17], while the rest span the signal subspace.
3. Assume the signal subspace is  $(J + 1)$  dimensional. Then, the basis vectors for the signal subspace, obtained from the eigendecomposition procedure, can be sorted in an  $M \times (J + 1)$  matrix  $\mathbf{E}_s$  with the column space identical to the signal subspace.
4. Project the cumulant-based steering vector estimate  $\mathbf{c}$ , on the signal subspace to obtain an improved estimate  $\mathbf{c}_{imp}$ , as

$$\mathbf{c}_{imp} = \mathbf{E}_s \mathbf{E}_s^H \mathbf{c}$$

5. Compute the weights for the beamformer, as

$$\mathbf{w}_{imp} = \mathbf{R}^{-1} \mathbf{c}_{imp}$$

### 4.3 Robustness Constraint

Any estimation procedure is inevitably subject to errors. MVDR beamforming is extremely sensitive to mismatch [24]-[30], especially in high SNR conditions and in arrays with large number of elements. A variety of constraints have been summarized in [6] assuming perfect knowledge of element characteristics and locations; however, in our case these methods are not applicable since there is no available information about the array manifold to design effective constraints.

Errors in the steering vector estimate result in signal cancellation. This mismatch condition, arising from non-perfect estimation, can be viewed as the problem of optimum beamforming with an array of sensors at slightly perturbed locations. In [35], a method that constrains the white noise gain of the processor is proposed for the solution of the latter problem. In this section, we use the same approach to alleviate the effects of estimation errors in cumulant-based optimum beamforming.

In order to understand the mismatch problem and find a way to alleviate its effects, we need to analyze the problem analytically. Consider the power response of a beamformer with a weight vector  $\mathbf{w}$ , as a function of DOA  $\theta$ , defined as

$$P(\theta) \triangleq |\mathbf{w}^H \mathbf{a}(\theta)|^2 \quad (4.2)$$

with  $\mathbf{a}(\theta)$  denoting the steering vector for an arrival from  $\theta$ . The derivative,  $\partial P(\theta)/\partial\theta$ , can be expressed, as

$$\frac{\partial P(\theta)}{\partial\theta} = 2\text{Re}\{ \mathbf{w}^H \mathbf{a}(\theta) [ \sum_{l=1}^M w_l \frac{\partial}{\partial\theta} a_l^H(\theta) ] \} \quad (4.3)$$

Now consider the following scenario: we have an MVDR processor *looking* at  $\theta_o$ , which is the

expected DOA for the desired signal. Instead, the source illuminates the array from  $\theta_d$  which is very close but not equal to  $\theta_o$ . In this case, the beamformer treats the desired signal as interference and nulls it; however, due to the distortionless response constraint for  $\theta_o$ , and since the angles are very close, the derivative  $\partial P(\theta)/\partial\theta$  must be large in magnitude for  $\theta$  between  $\theta_d$  and  $\theta_o$ . From the derivative expression (4.3), it is clear that this is possible only if the norm of the weight vector increases, since the inner product,  $\mathbf{w}^H \mathbf{a}(\theta)$ , and, the derivatives,  $\{\frac{\partial}{\partial\theta} a_l^H(\theta)\}_{l=1}^M$  are bounded. In this situation, the constraint is maintained by increasing the angle between the weight vector and the look-direction steering vector. This phenomena was exploited in [34], for tuning the beamformer to acquire a weak desired signal in the presence of strong interference.

Note that the white-noise amplification factor for any processor with a weight vector  $\mathbf{w}$  is  $\mathbf{w}^H \mathbf{w}$ ; hence, the nulling phenomena can be prevented if the white noise level at the processor is sufficiently high so that output power minimization criterion limits the increase in the norm of  $\mathbf{w}$ . This can be achieved by perturbing the covariance matrix estimate of array measurements by a scaled identity matrix as,

$$\mathbf{R}_p = \mathbf{R} + \epsilon \mathbf{I} \quad (4.4)$$

where  $\epsilon$  is a non-negative parameter which adjusts the strength of perturbation. Alternatively, it is possible to coin a term *virtual* SNR.  $\text{SNR}_v$ , defined as

$$\text{SNR}_v = \text{SNR} - 10 \log_{10} \left( \frac{\epsilon + \sigma_n^2}{\sigma_n^2} \right) \quad (4.5)$$

We then determine the weight vector as,

$$\mathbf{w} = \mathbf{R}_p^{-1} \mathbf{a}(\theta_o) \quad (4.6)$$

A recent method presented in [35] performs this procedure in an adaptive fashion by a simple scaling of the weight vector. In our case, we do not have source DOA information, but we do have an estimate of the steering vector. It is therefore possible to use this estimate in place of  $\mathbf{a}(\theta_o)$  in (4.6) to formulate the cumulant-based processor with limited signal nulling property.

## Chapter 5

# Multipath Phenomena

Eigendecomposition-based high-resolution methods [11]-[21] have proven to be effective means of obtaining bearing estimates of far-field narrowband sources from noisy measurements. The performance of these algorithms is severely degraded when coherence is present. Several methods have been proposed to solve the coherent signals problem with restrictions on array geometry [44]-[50]; however, with lack of knowledge of array manifold it is not possible to solve the coherence problem. MVDR beamforming also fails to perform optimally, when interference signals are correlated with the desired signal [51]-[52]. In some scenarios, even the conventional beamformer outperforms the MVDR approach due to signal cancellation in the MVDR beamformer.

In Chapter 3, we showed that the cumulant-based beamformer is not affected by the presence of coherence among interfering Gaussian signals as long as they are not correlated with the desired signal. The same is not possible for high-resolution DOA estimation methods; but, the MVDR beamformer may perform equally well if the desired signal steering vector is known and a satisfactory estimate of  $\mathbf{R}$  is available. In this chapter, we show that the cumulant-based approach is not affected by the presence of multipath propagation of the desired signal. In addition, we show that

the cumulant-based processor turns out to be the maximal-ratio-combiner [61] that maximizes the SINR.

With the presence of multipath propagation or smart jamming, our signal model in (2.1) changes to

$$r_k(t) = d(t) \sum_{l=1}^L a_k(\theta_{d_l}) \eta_l + \sum_{j=1}^J a_k(\theta_{i_j}) i_j(t) + n_k(t) \quad (5.1)$$

or in vector form

$$\mathbf{r}(t) = \begin{bmatrix} \mathbf{a}(\theta_{d_1}), \mathbf{a}(\theta_{d_2}), \dots, \mathbf{a}(\theta_{d_L}) \end{bmatrix} \begin{bmatrix} \eta_1 \\ \eta_2 \\ \vdots \\ \eta_L \end{bmatrix} d(t) + \mathbf{A}_I \mathbf{i}(t) + \mathbf{n}(t) \quad (5.2)$$

where the set of scalars  $\{ \eta_1, \eta_2, \dots, \eta_L \}$  constitute the multipath coefficients for an  $L$ -ray scenario.

The set of vectors,  $\{ \mathbf{a}(\theta_{d_1}), \mathbf{a}(\theta_{d_2}), \dots, \mathbf{a}(\theta_{d_L}) \}$  are the corresponding steering vectors of the  $L$ -ray model. Letting

$$\mathbf{b} \triangleq \begin{bmatrix} \mathbf{a}(\theta_{d_1}), \mathbf{a}(\theta_{d_2}), \dots, \mathbf{a}(\theta_{d_L}) \end{bmatrix} \begin{bmatrix} \eta_1 \\ \eta_2 \\ \vdots \\ \eta_L \end{bmatrix} = \mathbf{A}_D \boldsymbol{\eta} \quad (5.3)$$

we can reduce the signal model for multipath phenomena to the single-ray propagation model of Section 2.1,

$$\mathbf{r}(t) = \mathbf{b} d(t) + \mathbf{A}_I \mathbf{i}(t) + \mathbf{n}(t) \quad (5.4)$$

because we can view the vector  $\mathbf{b}$  as a *generalized* steering vector for a single desired signal although it may not be a vector in the array manifold. Therefore, following our work in Chapter 3, cumulant-based blind estimation procedure will yield

$$\mathbf{c} = \beta_4 \mathbf{b} \quad (5.5)$$

where  $\beta_4 = |b_1|^2 b_1^H \gamma_{d,4}$ , in which  $b_1$  is the first component of  $\mathbf{b}$ . Incorporating (5.5) into the constrained power minimization procedure, we obtain the following weight vector,

$$\mathbf{w}_{cum} = \beta_5 \mathbf{R}^{-1} \mathbf{c} = \beta_4 \beta_5 \mathbf{R}^{-1} \mathbf{b} \quad (5.6)$$

where  $\beta_5 = (\mathbf{c}^H \mathbf{R}^{-1} \mathbf{c})^{-1}$ .

Next, we find an alternate expression for  $\mathbf{w}_{cum}$ . Recall that the optimization problem which results in  $\mathbf{w}_{cum}$  is: minimize  $\mathbf{w}^H \mathbf{R} \mathbf{w}$  subject to  $\mathbf{w}^H \mathbf{c} = 1$ , or by (5.5),  $\mathbf{w}^H \mathbf{b} = 1/\beta_4$ . We can express the output power in the following way by using (2.9) and (5.4),

$$\mathbf{w}^H \mathbf{R} \mathbf{w} = \sigma_d^2 |\mathbf{w}^H \mathbf{b}|^2 + \mathbf{w}^H \mathbf{R}_u \mathbf{w} \quad (5.7)$$

but, due to the constraint  $\mathbf{w}^H \mathbf{b} = 1/\beta_4$ , the first term in the above expression is a constant. Therefore, the original optimization problem can be translated into : minimize  $\mathbf{w}^H \mathbf{R}_u \mathbf{w}$ , subject to  $\mathbf{w}^H \mathbf{c} = 1$  or equivalently,  $\mathbf{w}^H \mathbf{b} = 1/\beta_4$ . The solution to this problem is

$$\mathbf{w}_{cum} = \beta_6 \mathbf{R}_u^{-1} \mathbf{c} \quad (5.8)$$

where  $\beta_6 = (\mathbf{c}^H \mathbf{R}^{-1} \mathbf{c})^{-1}$ . Of course, this solution can also be expressed in terms of  $\mathbf{b}$ , as

$$\mathbf{w}_{cum} = \beta_7 \mathbf{R}_u^{-1} \mathbf{b} \quad (5.9)$$

where  $\beta_7 = \beta_4 \beta_6$ .

Note that although (5.8) and (5.9) are alternate expressions for  $\mathbf{w}_{cum}$ , they are not the way to actually compute  $\mathbf{w}_{cum}$ , since  $\mathbf{R}_u$  is not available in general.

Next, we determine the weight vector that yields the maximum SINR. SINR can be expressed as a function of the weight vector of the beamformer, as

$$\text{SINR}(\mathbf{w}) = \sigma_d^2 \frac{\mathbf{w}^H \mathbf{b} \mathbf{b}^H \mathbf{w}}{\mathbf{w}^H \mathbf{R}_u \mathbf{w}} \quad (5.10)$$

Defining,  $\mathbf{v} = \mathbf{R}_u^{1/2} \mathbf{w}$  so that  $\mathbf{w} = \mathbf{R}_u^{-1/2} \mathbf{v}$ , we can reexpress (5.10), as

$$\text{SINR}(\mathbf{w}) = \text{SINR}(\mathbf{R}_u^{-1/2} \mathbf{v}) = \sigma_d^2 \frac{|\mathbf{v}^H \mathbf{R}_u^{1/2} \mathbf{b}|^2}{\mathbf{v}^H \mathbf{v}} \quad (5.11)$$

Applying the Schwarz inequality [50] to (5.11), we find that

$$\text{SINR}(\mathbf{w}) = \text{SINR}(\mathbf{R}_u^{-1/2} \mathbf{v}) \leq \sigma_d^2 \|\mathbf{R}_u^{-1/2} \mathbf{b}\|^2 = \sigma_d^2 \mathbf{b}^H \mathbf{R}_u^{-1} \mathbf{b} \quad (5.12)$$

where equality holds if and only if

$$\mathbf{v} = \beta_8 \mathbf{R}_u^{-1/2} \mathbf{b} \quad (5.13)$$

in which  $\beta_8$  is a non-zero constant. Consequently, the optimum weight vector  $\mathbf{w}_{\text{SINR}}$ , which yields



the maximum SINR, can be determined from  $\mathbf{w} = \mathbf{R}_u^{-1/2} \mathbf{v}$  and (5.13), as

$$\mathbf{w}_{\text{SINR}} = \beta_8 \mathbf{R}_u^{-1} \mathbf{b} \quad (5.14)$$

Based on this derivation, some comments are in order. It is clear, by comparing (5.9) and (5.14), that the cumulant-based beamformer does indeed yield the maximum possible SINR, since  $\mathbf{w}_{\text{cum}}$  is just a scaled version of  $\mathbf{w}_{\text{SINR}}$ . This observation proves that the cumulant-based beamformer is optimal. In addition,  $\mathbf{w}_{\text{cum}}$  can be computed from the received data, whereas  $\mathbf{w}_{\text{SINR}}$ , as implemented in (5.14), requires knowledge of  $\mathbf{R}_u$ , which can not be determined from the received data in the presence of the desired signal. Finally, note that robust approaches presented in Chapter 4 are directly applicable in the presence of multipath.

## Chapter 6

# Adaptive Processing

In real-world applications, adaptive beamforming is an important requirement, especially when the desired signal source is in relative motion with respect to the array. In this chapter, we address this problem by providing an “estimate and plug” type of adaptive algorithm for the CUM<sub>1</sub> method.

The beamforming procedure (3.16) requires the inverse of the sample covariance matrix to compute the weights. We can estimate the covariance matrix recursively, as

$$\hat{\mathbf{R}}_t = (1 - \alpha_1)\hat{\mathbf{R}}_{t-1} + \alpha_1 \mathbf{r}(t)\mathbf{r}^H(t) \quad (6.1)$$

Since we need to propagate the inverse of  $\hat{\mathbf{R}}_t$ , we use the Sherman-Morrison formula [62], to obtain

$$\hat{\mathbf{R}}_t^{-1} = \frac{1}{1 - \alpha_1} \left[ \hat{\mathbf{R}}_{t-1}^{-1} - \alpha_1 \frac{\hat{\mathbf{R}}_{t-1}^{-1} \mathbf{r}(t) \mathbf{r}^H(t) \hat{\mathbf{R}}_{t-1}^{-1}}{1 - \alpha_1 [1 - \mathbf{r}^H(t) \hat{\mathbf{R}}_{t-1}^{-1} \mathbf{r}(t)]} \right] \quad t = 1, 2, \dots \quad (6.2)$$

with  $\hat{\mathbf{R}}_0^{-1} = \gamma \mathbf{I}$  where  $\gamma$  is a large positive number and  $\alpha_1$  controls the learning rate for second-order statistics.

To compute the weight vector, we also need the cumulant-based estimate of the source steering vector  $\mathbf{c}$ . We can estimate it recursively as

$$\hat{c}_l(t) = (1 - \alpha_2)\hat{c}_l(t-1) + \alpha_2[|r_1(t)|^2 r_1^H(t)r_l(t) - 2p(t)q(t) - v^H(t)x(t)] \quad (6.3)$$

with the auxiliary processes defined as

$$p(t) = (1 - \alpha_3)p(t-1) + \alpha_3|r_1(t)|^2$$

$$q(t) = (1 - \alpha_3)q(t-1) + \alpha_3 r_1^H(t)r_l(t)$$

$$v(t) = (1 - \alpha_3)v(t-1) + \alpha_3 r_1^2(t)$$

$$x(t) = (1 - \alpha_3)x(t-1) + \alpha_3 r_1(t)r_l(t)$$

The auxiliary processes are required in order to implement the cross-correlation terms in (3.11). The initial values for the auxiliary processes can be set to zero. Different learning rates are provided to emphasize the fact that higher-order statistics require longer periods to acquire the required information.

We can perform adaptive beamforming by computing the weight vector at each time as

$$\mathbf{w}(t) = \hat{\mathbf{R}}_t^{-1} \hat{\mathbf{c}}(t) \quad (6.4)$$

and obtain the array output, as

$$y(t) = \mathbf{w}^H(t)\mathbf{r}(t). \quad (6.5)$$

Adaptive versions of  $CUM_2$  and  $C^2$  methods will appear in a later publication.

## Chapter 7

# Simulations

In this chapter we present various experiments to illustrate the performance of cumulant-based beamforming. In all of the experiments we employed a uniformly spaced linear array, rather than an arbitrary geometry. This is done for two reasons: covariance-based techniques are mainly designed for this type of array structure, e.g., the spatial smoothing algorithm [44]- [50], so that it will be possible to compare both previous and future work with our current results. In addition, allowing a sufficient number of multipath rays, it is possible to represent any arbitrary steering vector by the linear array, since the steering vectors of the uniformly spaced isotropic linear array exhibit Vandermonde structure, resulting in linearly independent vectors for different DOA's. In all batch type of experiments, the record length is 1000 snapshots and the array has 10 isotropic elements with uniform half-wavelength spacing.

## 7.1 Experiment 1: Desired Signal in White-Noise

In this experiment, we employ the linear array described above for optimum reception of a BPSK signal, which is expected to arrive from broadside in the presence of temporally and spatially white, equal power, circularly symmetric sensor noise; however, the desired source illuminates the array from  $5^\circ$  broadside.

Our first MVDR beamformer,  $MVDR_1$ , looks to broadside, i.e., a mismatch condition. Our second MVDR beamformer,  $MVDR_2$ , uses exact knowledge of DOA of the desired signal. We also employ the cumulant-based beamformer of Chapter 3,  $CUM_1$ , and the improved cumulant-based beamformer  $CUM_2$  of Section 4.1. We investigate the performance of these processors for the following two elemental SNR levels: 20 dB for a strong signal and 0 dB for a weak signal. Note that the white-noise gain of any processor is limited to 10 dB by the number of sensors [35].

The beampattern responses (4.2), and white-noise gains of these beamformers are presented in Figure 7.1 for SNR=20 dB. All responses are normalized to have a maximum value of 0 dB. For comparison purposes, the optimum beamformer response, calculated by using true statistics in (3.16), is presented as the dashed curves. Observe that due to the mismatch condition,  $MVDR_1$  nulls the desired signal. More interestingly, the  $MVDR_2$  processor that utilizes the true DOA information does not improve the SNR, due to the mismatch arising from the use of a sample-data covariance matrix. The cumulant-based processors,  $CUM_1$  and  $CUM_2$ , yield excellent performance without any knowledge of source DOA. It is very important to observe that the performance of cumulant-based processors are better than that of the MVDR with exactly known look-direction.

We performed 100 Monte-Carlo runs to investigate the performance in a better way. The results are given in Table 7.1.

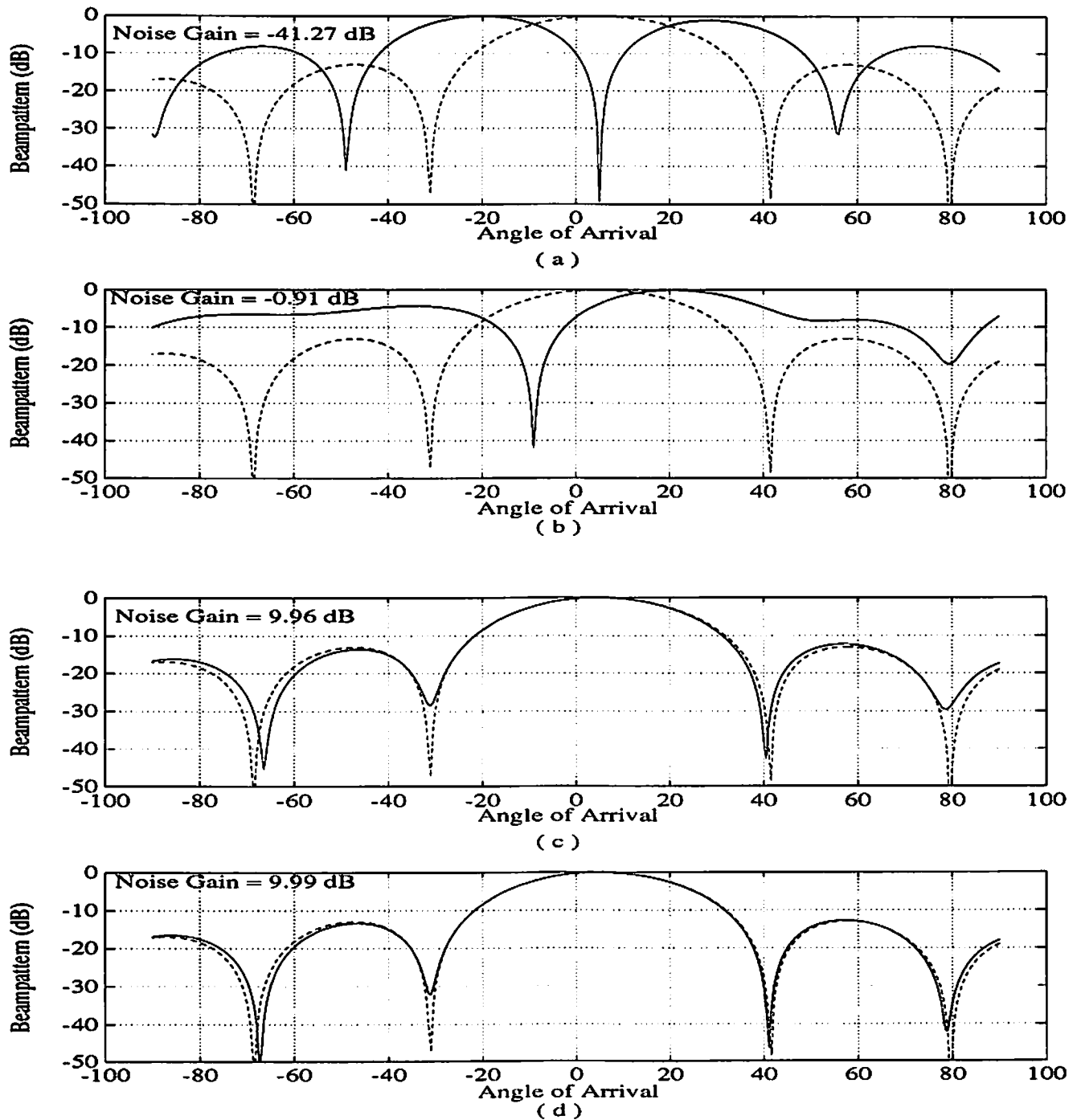


Figure 7.1: Beampatterns and white-noise gains of processors in a single realization for  $\text{SNR} = 20$  dB : (a)  $\text{MVDR}_1$ , (b)  $\text{MVDR}_2$ , (c)  $\text{CUM}_1$ , (d)  $\text{CUM}_2$ . The optimum pattern is illustrated in dashed lines for comparison purposes.

Table 7.1: Results from 100 Monte-Carlo Runs for Experiment 1

Processor	White-Noise Gain (dB)			
	SNR=20dB		SNR=0dB	
	Mean	Std.	Mean	Std.
MVDR <sub>1</sub>	-38.130	1.579	0.413	0.281
MVDR <sub>2</sub>	0.179	1.360	9.583	0.131
CUM <sub>1</sub>	9.954	0.015	9.058	0.359
CUM <sub>2</sub>	9.990	0.003	9.959	0.014

From these results, it is clear that cumulant-based processors are superior and the extra computation involved in CUM<sub>2</sub> reduces the variations. Note, also, that variations in the MVDR processors are significantly larger than those of the cumulant-based counterparts. This agrees with the previous remarks about the sensitivity of MVDR processing to experimental conditions in a high-SNR environment.

We performed the same experiment for 0 dB SNR condition. Figure 7.2 illustrates the beam-pattern responses and white-noise gains of the processors. Monte-Carlo results are also given in Table 7.1. In this low-SNR condition, MVDR results are expected to improve since the mismatch conditions for the desired signal will be masked by the presence of white noise of comparable power, as explained in Chapter 4. MVDR<sub>1</sub> processor does not offer a significant gain due to the persistent mismatch condition, but MVDR<sub>2</sub> yields a near-optimum result, since presence of higher-level noise masks the mismatch due to the use of a sample-covariance matrix. The performance of CUM<sub>1</sub> processor is slightly below than that of MVDR<sub>2</sub> and exhibits more variations. This is due to the inefficient use of the array data, since a high-level of noise corrupts the cumulant estimates and with CUM<sub>1</sub> there are no precautions to combat these errors. As expected, CUM<sub>2</sub> overcomes this problem by using SVD. Results in Table 7.1 indicate that CUM<sub>2</sub> achieves the best performance



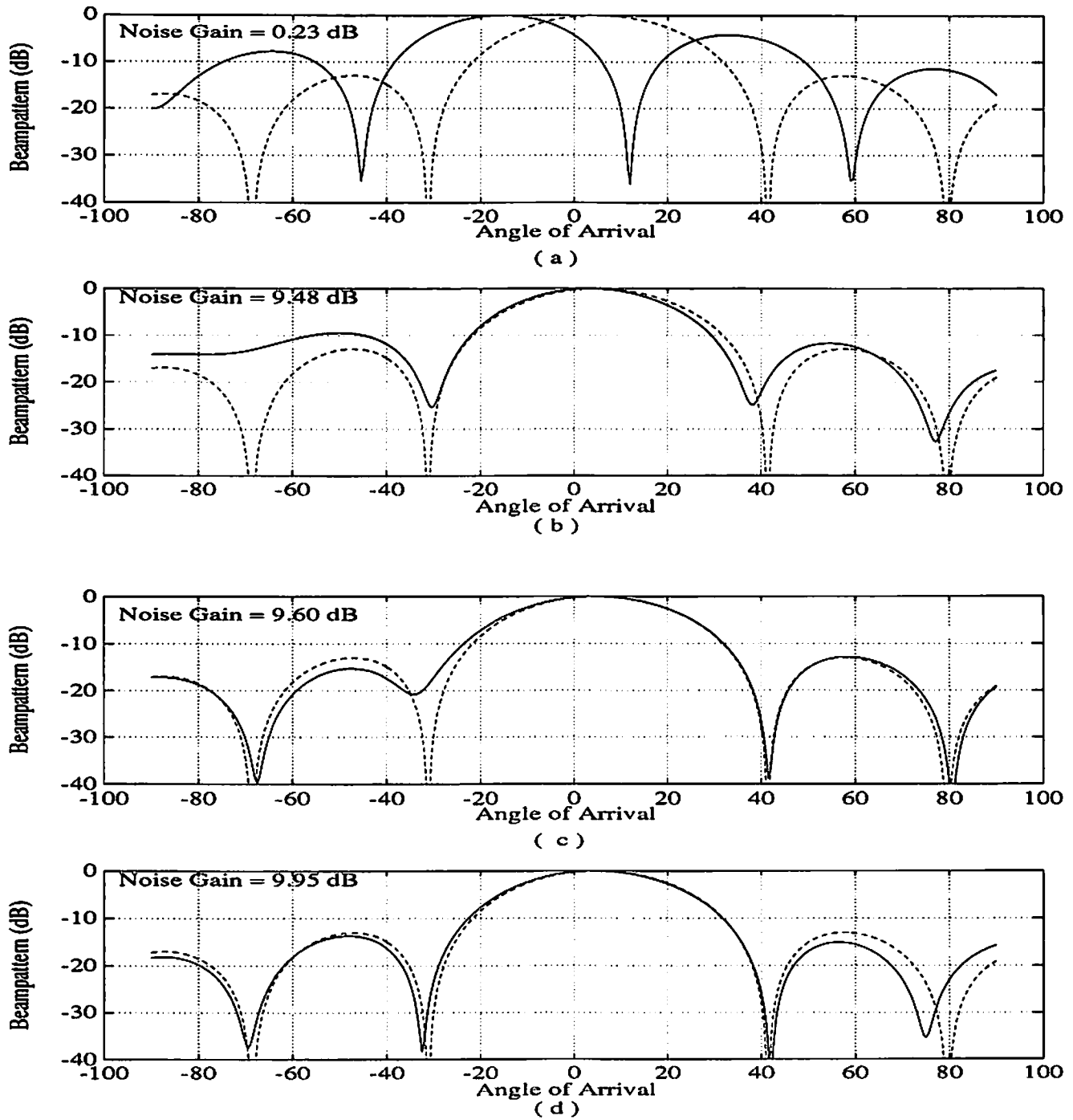


Figure 7.2: Beampatterns and white-noise gains of processors in a single realization for SNR = 0 dB : (a) MVDR<sub>1</sub>, (b) MVDR<sub>2</sub>, (c) CUM<sub>1</sub>, (d) CUM<sub>2</sub>. The optimum pattern is illustrated in dashed lines for comparison purposes.

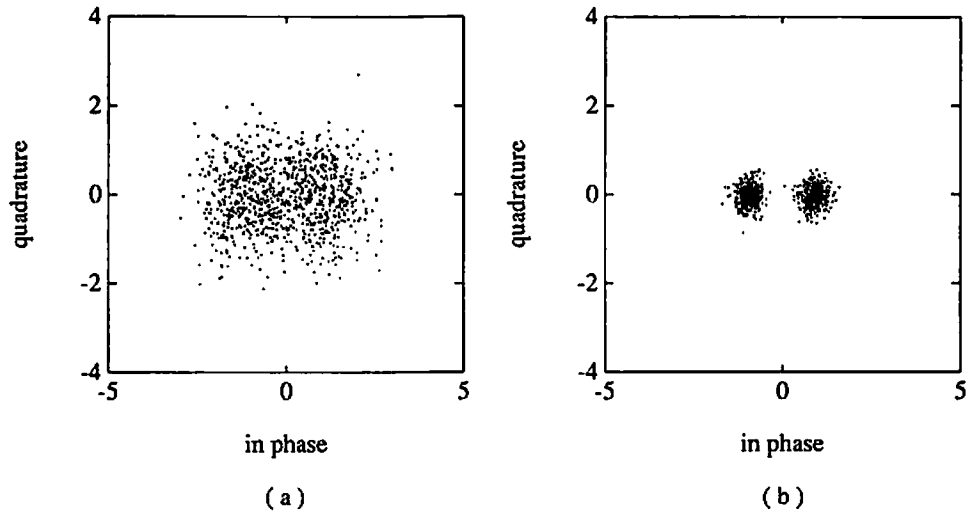


Figure 7.3: Power of cumulant-based beamforming: (a) received signal at the reference element at  $\text{SNR} = 0$  dB, (b) output of  $\text{CUM}_2$  processor.

with minimum variations.

Finally, to demonstrate the power of cumulant-based beamforming, we illustrate the received signal and the output of  $\text{CUM}_2$  processor for  $\text{SNR}=0$  dB case in Figure 7.3. It is clear that  $\text{CUM}_2$  is capable of sufficient noise rejection for performing correct decisions.

## 7.2 Experiment 2: Spatially Colored Noise and Multipath Propagation

In this experiment, we investigate the performance of the proposed approach in the presence of spatially colored noise. We employ the linear array of the previous experiment. We assume that the

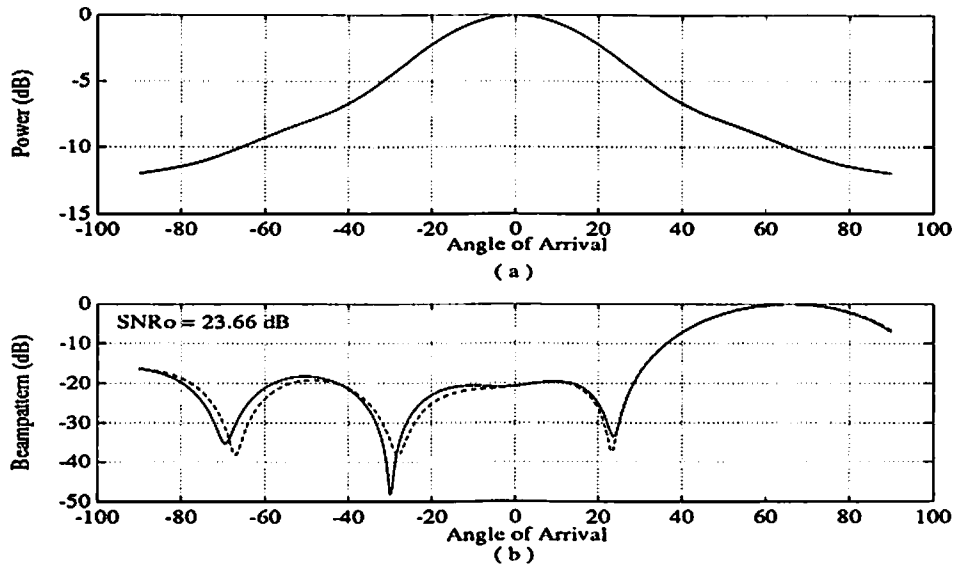


Figure 7.4: Beamforming in the presence of spatially colored noise: (a) Spatial Power Spectral Density of noise, (b) Beampattern of CUM<sub>2</sub> processor. The optimum pattern is illustrated in dashed lines for comparison purposes.

noise field is created by a set of point sources distributed symmetrically about the broadside of the linear array. As suggested in [63], this source structure is typical when the noise field is spherically or cylindrically isotropic. In this case, the noise covariance matrix is symmetric-Toeplitz. In our experiment, we use the following structure for the covariance matrix of undesired components,

$$\mathbf{R}_u(i, j) = 0.8^{|i-j|} \quad (7.1)$$

The spatial power spectrum of undesired components is illustrated in Figure 7.4a. It is clear that most of the noise leaks into the system from broadside. The desired signal illuminates the array from broadside, with an SNR of 10 dB. To illustrate the optimum combining property of our approach, we implanted an exact replica of the desired signal illuminating the array from 60°, where noise power is relatively less when compared to that from broadside. The beampattern of CUM<sub>2</sub>

Table 7.2: Results from 100 Monte-Carlo Runs for Experiment 2

Processor	SNR <sub>o</sub> (dB)	
	Mean	Std
CUM <sub>1</sub>	23.641	0.017
CUM <sub>2</sub>	23.645	0.015

processor is given in Figure 7.4b. For comparison purposes, we present the response of the optimum beamformer based on exact statistical information, as a dashed curve. The maximum-possible SNR at the output is 23.689 dB for this scenario. It is clear that the response of CUM<sub>2</sub> is almost identical to that of the optimum beamformer: both processors emphasize the signal illuminating the array from 60°, since the noise contribution is less in this region. We performed 100 Monte-Carlo runs for this scenario, and the results are presented in Table 7.2. It is clear that both cumulant-based processors perform equally well. The reason for this phenomenon is the presence of the multipath from 60° through a low-noise background that virtually increases the effective SNR, which, in turn, alleviates the effects of estimation errors. Note that the peak of the beampattern is slightly shifted from 60°, in order to receive less interference. Similar behavior is observed in covariance-based direction-of-arrival estimation in the presence of colored noise resulting in biased estimates of parameters.

### 7.3 Experiment 3: Effects of Robustness Constraint

In this experiment, we illustrate the effects of the robustness constraint of Section 4.3, on a CUM<sub>1</sub> processor in the presence of white noise. We employ the same array as in the previous experiments. We employ CUM<sub>1</sub>, since this processor uses the data inefficiently, and requires a robust approach. In our experiment, we consider the situation with SNR=0 dB. Figure 7.5 illustrates the beampatterns

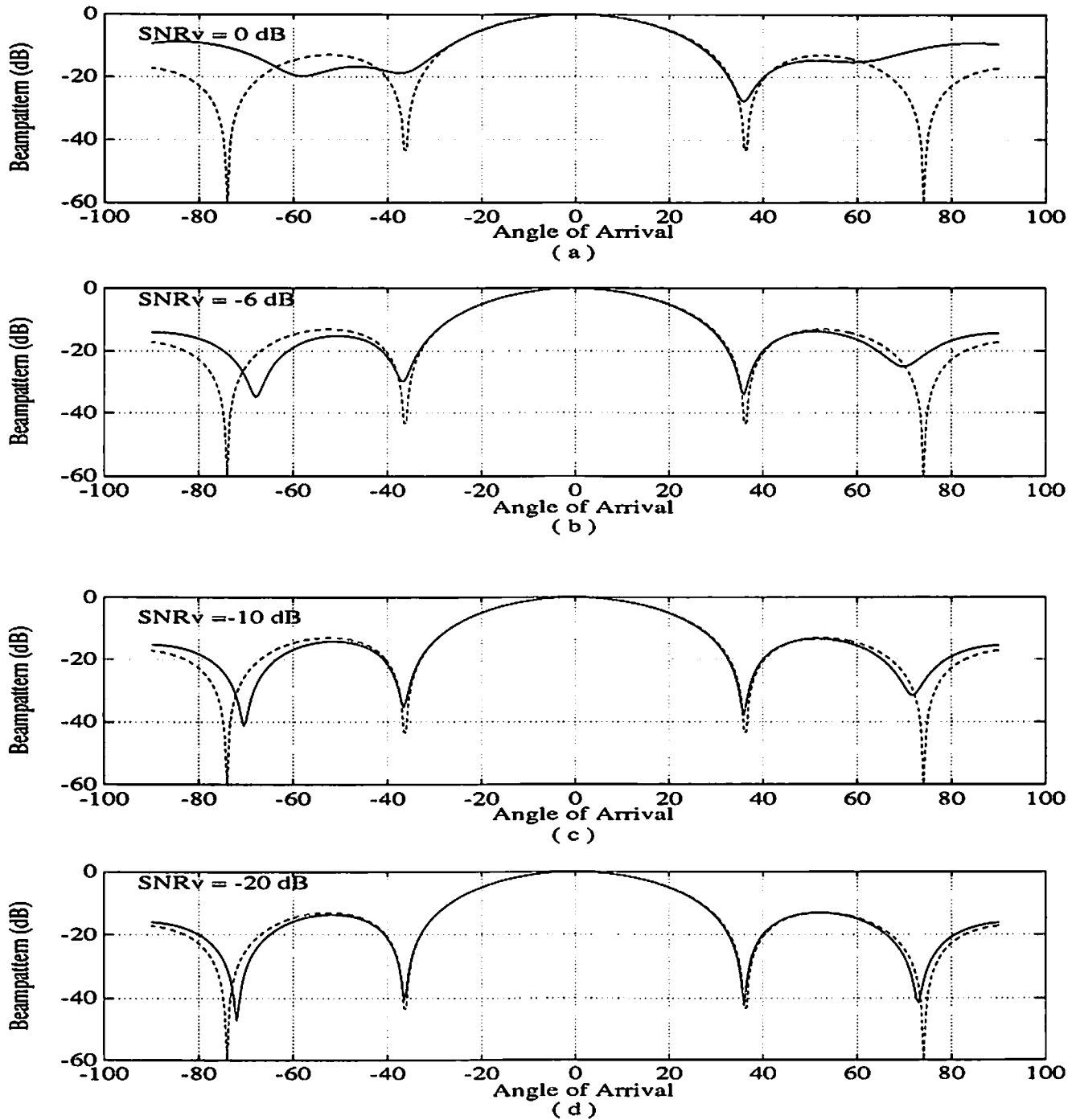


Figure 7.5: Beam pattern of  $CUM_1$  processor for varying virtual SNR: (a) 0 dB, (b) -6 dB, (c) -10 dB, (d) -20 dB. The optimum pattern is illustrated in dashed lines for comparison purposes.

of  $CUM_1$  processor for several  $SNR_v$  values. It is clear from the results that, as the perturbation increases, the patterns match better since the mismatch due to estimation errors in the steering vector estimate are masked by the presence of virtual increased level of noise. This method should be used sparingly in the presence of jammers, because increasing the virtual noise level results in diverting the capability of the array from nulling the directional interference.

## 7.4 Experiment 4: Multiple Interferers

In this experiment, we consider the problem of beamforming in a multipath environment in the presence of multiple jammers. We employ the same array as in the previous experiments. The signal of interest originates from a BPSK communication source, and it is expected from broadside; however, due to multipath effects, multiple delayed and shifted replicas are received. There are two jammers, and one is subject to multipath as well. Table 7.3 summarizes the signal structure. Note that there are 10 wavefronts illuminating the array and it is not possible to estimate their

Table 7.3: Signal structure for Experiment 4

Source	Power (dB)	Multipath Coeff.	DOA
BPSK	10	(0.0,-0.5)	$-10^\circ$
		(0.9895,-0.0311)	$-2^\circ$
		(1.0,0.0)	$0^\circ$
		(-0.6472,-0.4702)	$6^\circ$
		(-0.8,0.0)	$8^\circ$
		(0.1414,0.1414)	$11^\circ$
		(0.0462,0.0191)	$18^\circ$
JAMMER <sub>1</sub>	10	(1.0,0.0)	$26^\circ$
		(0.5657,0.5657)	$32^\circ$
JAMMER <sub>2</sub>	10	(1.0,0.0)	$-1^\circ$
NOISE	0	—	—

DOA's with any existing high-resolution method; hence, signal-COPY algorithms [17] can not be

used even with perfect knowledge of the array manifold.

Due to presence of coherent wavefronts, second-order statistics are not spatially stationary along the array; hence, it is not meaningful to define SINR at an array element. Instead, we compute the SINR at the output of the optimal processor by employing true statistics. The maximum possible  $\text{SINR}_o$  is found from (5.12) to be 12.677 dB. From Table 7.4, we observe that  $\text{CUM}_2$  performs very well under these severe conditions. Performance of  $\text{CUM}_1$  is effected by strong interferers since this processor does not utilize all of the available information. Finally, we observe that MVDR with correct look-direction cancels the desired signal due to coherence. Note that  $\text{CUM}_2$  exhibits less variations than other processors.

To gain more insight into the operation of the processors, we illustrate the beampatterns for MVDR and  $\text{CUM}_2$  in Figure 7.6. We focus on the region where the wavefronts are received by the array. It is observed that the MVDR processor does not null the jammer from  $-1^\circ$ , since it maintains the look-direction constraint for  $0^\circ$  and tries to minimize the output power by destructively combining the coherent wavefronts. On the other hand,  $\text{CUM}_2$  is blind to Gaussian interferers, and, as in Experiment 2, it estimates the *generalized* steering vector of the desired signal and combines the wavefronts to enhance SINR at the output.  $\text{CUM}_2$  puts a null on the jammer from  $-1^\circ$ , destructively combines the wavefronts from the first jammer by weight-phasing rather than

Table 7.4: Results from 100 Monte-Carlo Runs for Experiment 4

Processor	$\text{SINR}_o$ (dB)	
	Mean	Std
MVDR	-28.424	4.405
$\text{CUM}_1$	4.110	2.118
$\text{CUM}_2$	10.290	0.746
$C^2$	11.879	0.627

null-steering, and reinforces the wavefronts from the desired source.

Finally, we implemented the  $C^2$  beamformer suggested in Section 4.2: we first estimated the steering vector as done for  $CUM_2$ , but then further projected it into the subspace spanned by the principal eigenvectors of the sample covariance matrix. We used the resultant vector as the estimate of the desired signal steering vector, and constructed an MVDR beamformer based on it. The performance of the resultant processor is demonstrated in Table 7.4.

We observe that by combining cumulants with covariance information, we obtain the best results.

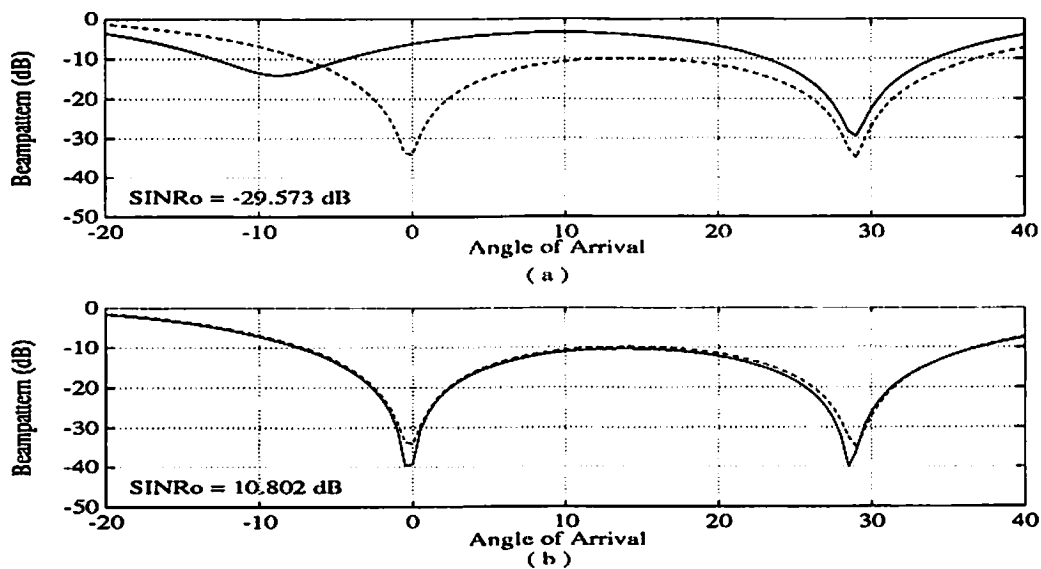


Figure 7.6: Beam patterns and array gains of processors: (a) MVDR with correct look direction, (b)  $CUM_2$ . The optimum pattern is illustrated in dashed lines for comparison purposes.

## 7.5 Experiment 5: Adaptive Processing

In this experiment, we demonstrate the results from the adaptive version of  $CUM_1$  approach as described in Chapter 6. We employed the 10 element uniform linear array of previous experiments.



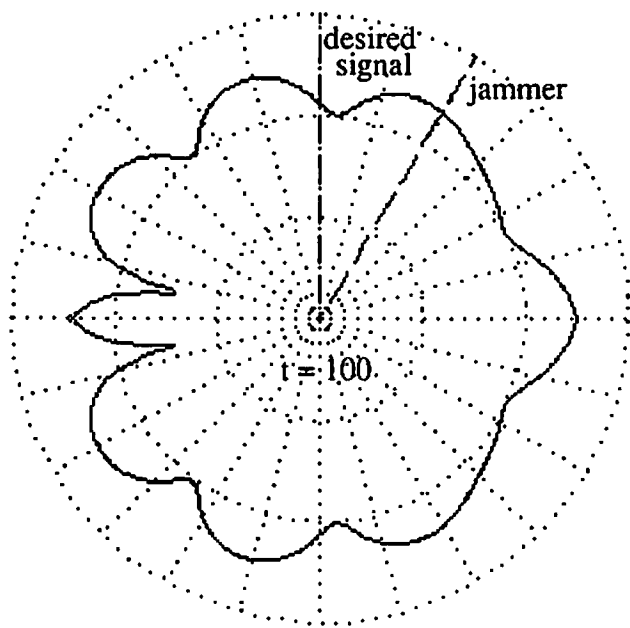
The initial pattern of the beamformer is designed to be isotropic, by letting  $\mathbf{c}(0) = [1, 0, \dots, 0]^T$ . Desired signal illuminates the array from broadside with SNR=10 dB. A jammer with power equal to that of the desired source is present at  $30^\circ$ . Note that there is no nonstationarity involved in this experiment; our aim is to demonstrate the evolution of the beamforming process and indicate the data lengths required for cumulant and covariance estimation. Tracking properties will be included in our future work, including comparisons with adaptive versions of CUM<sub>2</sub> and C<sup>2</sup> processors.

Figure 7.7 illustrates the beampattern of the adaptive CUM<sub>1</sub> processor as time evolves. After 100 snapshots, the beampattern is still close to isotropic. At 300 snapshots, covariance matrix estimate is improved, indicating the presence of desired signal from broadside. At this time point, the cumulant-based steering vector estimate has not matured, so it can not prevent the desired signal from being cancelled. After 500 snapshots, cumulant estimates get better, and there is a tendency to cancel the interference rather than the desired signal. Finally, after 700 snapshots the processor removes the interference by null steering.

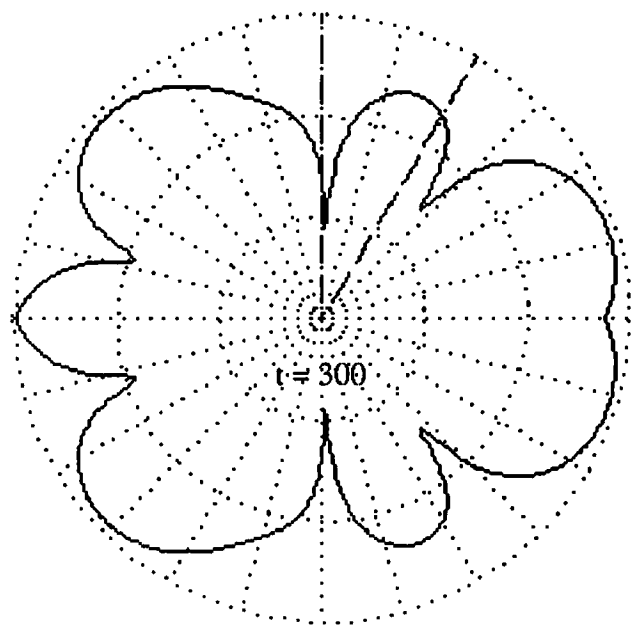
## 7.6 Experiment 6: Effects of Data Length

In this experiment, we employ the linear array of Experiment 1, with the same noise conditions, and vary the data length to observe the behavior of the beamformers CUM<sub>1</sub>, CUM<sub>2</sub>, MVDR<sub>1</sub> and MVDR<sub>2</sub>. Figure 7.8 demonstrates the variation of white-noise gain of the processors with data length, for 0 dB and 20 dB SNR levels. Each point on the plots is obtained by averaging the results from 50 Monte-Carlo simulations.

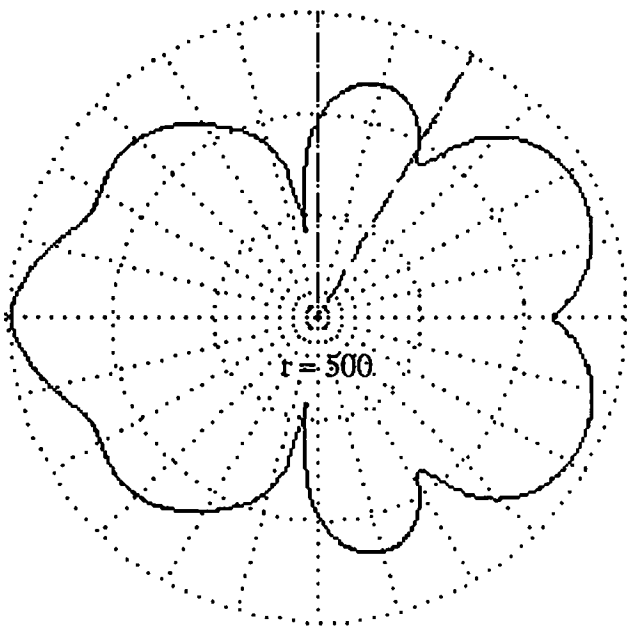
From Figure 7.8a it is clear that CUM<sub>2</sub> outperforms all the processors, including MVDR<sub>2</sub> which utilizes the correct look direction for all data lengths. Furthermore, small sample properties



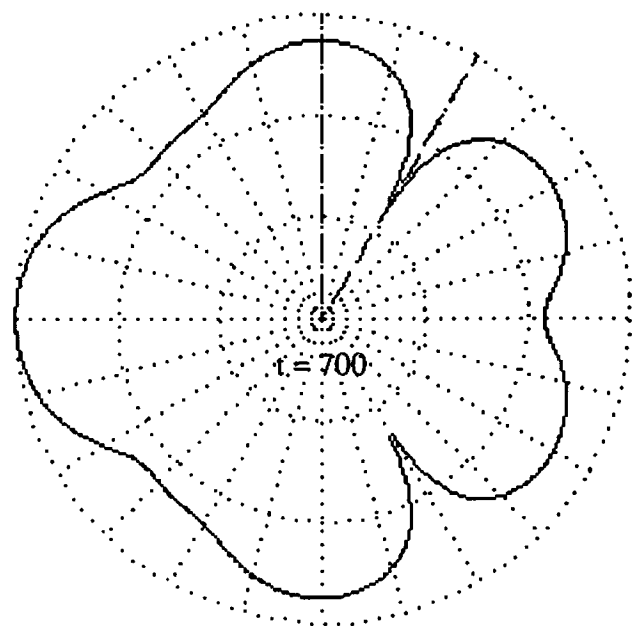
(a)



(b)



(c)



(d)

Figure 7.7: Beam pattern of the adaptive  $CUM_1$  processor as a function of time: desired signal is from broadside and the jammer is from  $30^\circ$  as indicated. (a)  $t=100$ , (b)  $t=300$ , (c)  $t=500$ , (d)  $t=700$ .

of  $CUM_2$  are quite impressive, motivating further research for developing its adaptive version. Low SNR masks the mismatch in  $MVDR_2$  due to the use of sample covariance matrix; hence, as can be seen from Figure 7.8a,  $CUM_1$  is inferior to  $MVDR_2$ .

Figures 7.8b and 7.8c, indicate the effect of higher SNR on performance.  $CUM_1$  and  $CUM_2$  perform almost identical for all data lengths. Their gain is larger than 9 dB even for less than 50 snapshots.  $MVDR_2$  can not recover in this experiment since the mismatch results in severe signal cancellation. We do not include the response of  $MVDR_1$ , because its performance drifts around -35 dB.

These results indicate that our approach has very *promising small sample behavior* that *deserves more research*. This will be a topic of another report.

**USC-SIPI REPORT #195**

**Cumulant-Based Blind Optimum  
Beamforming**

**by**

**Mithat C. Dogan and Jerry M. Mendel**

**January 1992**

**Signal and Image Processing Institute  
UNIVERSITY OF SOUTHERN CALIFORNIA  
Department of Electrical Engineering-Systems  
3740 McClintock Avenue, Room 404  
Los Angeles, CA 90089-2564 U.S.A.**

## Abstract

Sensor response, location uncertainty and use of sample statistics can severely degrade the performance of optimum beamformers. In this report, we propose blind estimation of the source steering vector in the presence of multiple, directional, correlated or coherent Gaussian interferers via higher-order-statistics. In this way, we employ the statistical characteristics of the desired signal to make the necessary discrimination, without any a-priori knowledge of array manifold and direction-of-arrival information about the desired signal. We then improve our method to utilize the data in a more efficient manner. In any application, only sample statistics are available, so we propose a robust beamforming approach that employs the steering vector estimate obtained by cumulant-based signal processing. We further propose a method that employs both covariance and cumulant information to combat finite sample effects. We analyze the effects of multipath propagation on the reception of the desired signal. We show that even in the presence of coherence, cumulant-based beamformer still behaves as *the* optimum beamformer that maximizes the Signal to Interference plus Noise Ratio (SINR). Finally, we propose an adaptive version of our algorithm. Simulations demonstrate the excellent performance of our approach in a wide variety of situations.

# Contents

<b>1</b>	<b>Introduction</b>	<b>1</b>
<b>2</b>	<b>Problem Formulation</b>	<b>4</b>
2.1	Signal Model . . . . .	4
2.2	Covariance-Based Approaches . . . . .	6
<b>3</b>	<b>Cumulant-Based Optimum Beamforming</b>	<b>10</b>
3.1	Higher-Order Statistics: Definitions and Properties . . . . .	11
3.2	Estimation of desired signal steering vector . . . . .	14
3.3	Interference Rejection . . . . .	15
<b>4</b>	<b>Robust Beamforming</b>	<b>17</b>
4.1	Efficient Utilization of Array Data . . . . .	17
4.2	Covariance-Cumulant ( $C^2$ ) Approach . . . . .	18
4.3	Robustness Constraint . . . . .	20
<b>5</b>	<b>Multipath Phenomena</b>	<b>23</b>
<b>6</b>	<b>Adaptive Processing</b>	<b>28</b>

<i>CONTENTS</i>	iii
<b>7 Simulations</b>	<b>31</b>
7.1 Experiment 1: Desired Signal in White-Noise . . . . .	32
7.2 Experiment 2: Spatially Colored Noise and Multipath Propagation . . . . .	36
7.3 Experiment 3: Effects of Robustness Constraint . . . . .	38
7.4 Experiment 4: Multiple Interferers . . . . .	40
7.5 Experiment 5: Adaptive Processing . . . . .	42
7.6 Experiment 6: Effects of Data Length . . . . .	43
<b>8 Conclusions</b>	<b>47</b>
<b>Appendix</b>	<b>48</b>
<b>A Third-order statistics based estimation</b>	<b>48</b>
<b>B Full utilization of array data</b>	<b>50</b>

# List of Figures

- 7.1 Beampatterns and white-noise gains of processors for SNR=20 dB . . . . . 33
- 7.2 Beampatterns and white-noise gains of processors for SNR=0 dB . . . . . 35
- 7.3 Power of cumulant-based beamforming . . . . . 36
- 7.4 Beamforming in the presence of spatially colored noise . . . . . 37
- 7.5 Beampattern of CUM<sub>1</sub> processor for varying virtual SNR . . . . . 39
- 7.6 Beampatterns and array gains of processors . . . . . 42
- 7.7 Beampattern of the *adaptive* CUM<sub>1</sub> processor as a function of time . . . . . 44
- 7.8 Performance of processors with varying data length . . . . . 46



# List of Tables

7.1	Results from 100 Monte-Carlo Runs for Experiment 1 . . . . .	34
7.2	Results from 100 Monte-Carlo Runs for Experiment 2 . . . . .	38
7.3	Signal structure for Experiment 4 . . . . .	40
7.4	Results from 100 Monte-Carlo Runs for Experiment 4 . . . . .	41

# Chapter 1

## Introduction

Array processing techniques play an important role in enhancement of signals in the presence of interference. A number of books, and an extensive literature [1]–[9] have already been published. Capon’s minimum-variance distortionless response (MVDR) beamformer [10] has been a starting point for both signal enhancement and high-resolution direction-of-arrival (DOA) estimation.

In recent years, there has been an increasing interest in high-resolution array processing techniques based on eigendecomposition of the covariance matrix of received signals [11]–[21]. To recover the signal of interest in the presence of interfering signals, the so-called COPY function [17] is used. In this procedure, DOA’s for all signals are first estimated, and then the minimum-variance processor that reconstructs the desired signal and minimizes the contribution of all interference sources is implemented. All of the previously referenced methods rely on complete knowledge of responses and locations of array elements and/or DOA information of the desired signal.

If the array manifold is unknown, or there are uncertainties, it is then necessary to calibrate the array [22]–[23]; however, this is not a practical thing to do, since calibration must be done quite frequently, and, each time, array-manifold information must be stored. In addition, calibration

sources may be required. Even small errors in the calibration procedure may considerably degrade the performance. Sensitivity analyses of high-resolution methods and MVDR beamforming have been presented in [24]–[32].

In this report, we shall employ higher-order statistics of received signals to estimate the steering vector of the non-Gaussian desired signal in the presence of directional Gaussian interferers with unknown covariance structure. We assume no knowledge of array manifold and DOA information about the desired signal. Desired signal may be voiced speech, sonar signal, radar return or a communication signal. In our work, we specialize to the communications scenario, which requires the use of fourth-order cumulants. Following a mathematical formulation of the problem in Chapter 2, we describe basic properties of cumulants and blind estimation and optimum beamforming procedures in Chapter 3.

Any estimation procedure is subject to errors, as is our cumulant-based source steering vector estimation method. In theory, cumulants are blind to Gaussian noise; however, their estimates are corrupted by such noise. In order to obtain satisfactory results, longer data lengths are necessary in cumulant-based signal processing. To alleviate the effects of estimation error in the beamforming step, we propose a more efficient estimation procedure that fully utilizes the data acquired by the array. We further suggest a method of combining cumulant and covariance information to yield better estimates. Then we employ a robust beamforming method based on artificial noise injection to combat mismatch in the source steering vector. We consider the estimation error as a mismatch and successfully apply this robust approach to our problem. These methods are presented in Chapter 4.

In a communications environment, multipath propagation almost always take place. In this case, all eigendecomposition-based techniques and MVDR fail. Only in some specific array configurations

is it possible to decorrelate incoming signals and then estimate their DOA's. We analyze the behavior of our cumulant-based approach in Chapter 5. We show that our proposed approach behaves as *the* optimum beamformer that maximizes the Signal to Interference plus Noise Ratio (SINR).

For real-time operation (a necessary requirement in communications applications) we propose an adaptive implementation of the cumulant-based beamformer in Chapter 6. We then present simulation experiments to indicate the performance of our approach in Chapter 7. Finally, we draw our conclusions in Chapter 8.

## Chapter 2

# Problem Formulation

We formulate our problem in a narrowband fashion. In array processing, a problem is classified as narrowband if the signal bandwidth is small compared to the reciprocal of the time required for the signal wavefront to propagate across the array. For a discussion on bandwidth, see [36]-[37].

In our formulation, lower and upper case italic letters are used to represent scalars, lower case bold-faced letters are used for vectors, and, upper case bold-faced letters are used for matrices.

### 2.1 Signal Model

Consider an array of  $M$  elements, with arbitrary sensor response characteristics and locations. Assume there are  $J$  Gaussian interference signals  $\{ i_j(t), j = 1, 2, \dots, J \}$ , and a non-Gaussian desired signal  $d(t)$ , centered at frequency  $w_o$ . We assume sources are far away from the array so that a planar wavefront approximation is possible. The additive noise present is assumed to be Gaussian with unknown covariance. With these assumptions, the received signal at the  $k$ th sensor can be expressed, as

$$r_k(t) = a_k(\theta_d) d(t) + \sum_{j=1}^J a_k(\theta_{i_j}) i_j(t) + n_k(t) \quad (2.1)$$

where,

- $\theta_x$  : the direction-of-arrival of the wavefront corresponding to emitter  $x$ .
- $a_k(\theta_x)$  : response of the  $k$ th sensor to  $x$ th signal wavefront, including the phase factor associated with the travel time of the signal wavefront with respect to a reference point; without loss of generality, this point can be taken as the first sensor location.
- $d(t)$  : the desired non-Gaussian signal as received at sensor 1, with variance  $\sigma_d^2$ .
- $i_j(t)$  : the  $j$ th interferer waveform as received at sensor 1; interference signals are assumed to be independent of the desired signal, and they are Gaussian processes.
- $n_k(t)$  : the additive noise at the  $k$ th sensor.

Equation (2.1) can be rewritten in matrix notation, as

$$\begin{bmatrix} r_1(t) \\ r_2(t) \\ \vdots \\ r_M(t) \end{bmatrix} = \begin{bmatrix} \mathbf{a}(\theta_d), \mathbf{a}(\theta_{i_1}), \dots, \mathbf{a}(\theta_{i_J}) \end{bmatrix} \begin{bmatrix} d(t) \\ i_1(t) \\ \vdots \\ i_J(t) \end{bmatrix} + \begin{bmatrix} n_1(t) \\ n_2(t) \\ \vdots \\ n_M(t) \end{bmatrix} \quad (2.2)$$

where  $\mathbf{a}(\theta_x)$  represents the  $M \times 1$  steering vector for the wavefront from emitter  $x$ , which can be expressed as

$$\mathbf{a}(\theta_x) = \begin{bmatrix} a_1(\theta_x), a_2(\theta_x), \dots, a_M(\theta_x) \end{bmatrix}^T \quad (2.3)$$

We define the *array manifold* as the collection of steering vectors over all DOA's of interest. Alternative expressions for the received signal vector are,

$$\mathbf{r}(t) = \mathbf{A} \mathbf{z}(t) + \mathbf{n}(t) = \mathbf{a}(\theta_d) d(t) + \mathbf{A}_I \mathbf{i}(t) + \mathbf{n}(t) \quad (2.4)$$

In this last expression, we partitioned the  $M \times (J + 1)$  steering matrix  $\mathbf{A}$  as,

$$\mathbf{A} = \left[ \mathbf{a}(\theta_d), \mathbf{A}_I \right] \quad (2.5)$$

where the  $M \times J$  matrix  $\mathbf{A}_I$ , is the steering matrix for interference sources.

In this report, we address the problem of optimum beamforming with an array of sensors whose responses and locations are completely unknown; hence, although we may have a priori knowledge about the direction-of-arrival of desired signal, we can not perform beamforming due to the lack of knowledge of array manifold. In [38], this problem is addressed; however, [38]'s algorithm is limited to a single interference signal. We investigate the possibility of a more general solution; namely, signal recovery in the presence of multiple interferers whose correlation structure is unknown. Before presenting our approach, which employs higher-order statistics, we demonstrate the limitations of covariance-based array processing for this problem.

## 2.2 Covariance-Based Approaches

Currently used high-resolution methods of DOA estimation and minimum-variance distortionless response beamforming (MVDR) employ the covariance matrix of signals received by the array. The wavefront covariance matrix,  $\mathbf{S}$ , is defined as the covariance of the source signals as received at the

reference point, i.e., at sensor 1:

$$\mathbf{S} = \mathcal{E} \{ \mathbf{z}(t) \mathbf{z}^H(t) \} \quad (2.6)$$

where  $(\cdot)^H$  denotes complex conjugate transpose. Using the received signal model in (2.4), we can express the  $M \times M$  covariance matrix  $\mathbf{R}$  of array measurements in the following two ways:

$$\mathbf{R} = \mathcal{E} \{ \mathbf{r}(t) \mathbf{r}^H(t) \} = \mathbf{A} \mathbf{S} \mathbf{A}^H + \mathbf{R}_n = \sigma_d^2 \mathbf{a}(\theta_d) \mathbf{a}^H(\theta_d) + \mathbf{R}_u \quad (2.7)$$

where  $\mathbf{R}_n$  is the noise covariance matrix,

$$\mathbf{R}_n = \mathcal{E} \{ \mathbf{n}(t) \mathbf{n}^H(t) \} \quad (2.8)$$

and,  $\mathbf{R}_u$  is the covariance matrix of the undesired signals, i.e.,

$$\mathbf{R}_u = \mathcal{E} \{ [ \mathbf{A}_I \mathbf{i}(t) + \mathbf{n}(t) ] [ \mathbf{A}_I \mathbf{i}(t) + \mathbf{n}(t) ]^H \} \quad (2.9)$$

In general, the noise covariance matrix,  $\mathbf{R}_n$ , is unknown. With some restrictions on array orientation and noise covariance structure, some approaches for high resolution DOA estimation are proposed in [39]-[40] that do not require this information; however, these techniques have their limitations due to involved assumptions. Even with complete knowledge of noise covariance structure, source localization is still impossible without the knowledge of array manifold. In [20], ESPRIT algorithm is devised to overcome this problem; however, ESPRIT requires transitionally equivalent subarrays with known displacement vectors, which may also be impractical due to all the constraints on array orientation. In [33], an eigendecomposition-based beamforming approach



is proposed which assumes the identifiability of the signal subspace and availability of the steering vector information for the signal of interest. Good results were obtained under these assumptions; however, this method can not handle coherent interference and spatially colored noise.

In [41]-[43], blind estimation of steering vectors for independent emitters is discussed with the following conclusion:

Blind estimation of source steering vectors is not possible with only second-order statistics, but employing higher-than-second-order cumulants, it is possible to estimate source steering vectors up to a scale factor.

MVDR beamforming is an alternate approach for signal recovery. This approach however, requires knowledge of the steering vector for the desired source up to a scale factor and uses the covariance matrix  $\mathbf{R}$  of received signals for processing. The output of the MVDR beamformer  $y(t)$  can be expressed as [10]

$$y(t) = \mathbf{w}^H \mathbf{r}(t) = [\beta_1 \mathbf{R}^{-1} \mathbf{a}(\theta_d)]^H \mathbf{r}(t) \quad (2.10)$$

where the constant  $\beta_1$  is present to maintain a specified response for the desired signal and  $\mathbf{w}$  denotes the weight vector of the processor.

From the above expression, it is clear that MVDR beamforming requires knowledge of  $\mathbf{a}(\theta_d)$ . Without knowledge of array manifold, it is not possible to determine  $\mathbf{a}(\theta_d)$  even in the case of known  $\theta_d$ . Therefore, MVDR beamforming can not be directly applied to our problem. In addition, the MVDR beamformer is quite sensitive to errors in assumed sensor locations and characteristics [24]-[29].

In many applications, multipath propagation takes place resulting in coherent sources. Coher-

ence presents a serious problem to DOA methods; it leads to a singular source covariance matrix  $\mathbf{S}$ , for which it is not possible to estimate source locations except in some specific array configurations [44]-[50]. In the MVDR case, source coherency does not represent a problem as long as there is no source correlated with the desired signal; however, this situation is rarely met in practice. In general, the desired signal is subject to multipath propagation, and performance of MVDR approach degrades severely [51]-[52]. An optimum beamforming procedure has been suggested in [53] to overcome the coherence problem by using a linear array of elements with identical directional characteristics.

We are therefore looking for a method that can overcome all these problems. In the next chapter, we present an approach that accomplishes this by combining cumulant-based blind estimation and MVDR beamforming.

## Chapter 3

# Cumulant-Based Optimum

# Beamforming

In the previous chapter, we discussed the problem of optimum beamforming and concluded that it is not possible to recover a desired signal in the presence of multiple interferers, unknown sensor noise covariance, and multipath propagation without any information about array manifold. In this chapter, we propose a method to overcome these problems. We propose a two-step procedure: higher-order-statistics for blind estimation of the source steering vector, followed by MVDR beamforming based on second-order statistics of received signals and steering vector estimate provided by the first step. Before describing our method we first present a brief review of higher-order statistics.

### 3.1 Higher-Order Statistics: Definitions and Properties

Let  $\{x_1, x_2, \dots, x_n\}$  be a collection of random variables and  $\{v_1, v_2, \dots, v_n\}$  be a collection of deterministic variables. We can stack these variables in vectors  $\mathbf{x} = [x_1, x_2, \dots, x_n]^T$  and  $\mathbf{v} = [v_1, v_2, \dots, v_n]^T$ . Then, the  $n$ th-order cumulant of the random variables is defined as the coefficient of  $(v_1, v_2, \dots, v_n)$  in the Mac-Laurin series expansion of the cumulant-generating function

$$K_{\mathbf{x}}(\mathbf{v}) = \ln ( E \{ \exp [ j \mathbf{v}^T \mathbf{x} ] \} ) \quad (3.1)$$

An alternate approach that defines the  $n$ th-order cumulant in terms of a weighted sum of joint moments of orders up to  $n$  is provided in [55].

For zero-mean real random variables, which we frequently encounter in applications, the second-, third-, and fourth-order cumulants are expressed, as

$$cum(x_1, x_2) = E \{ x_1 x_2 \}$$

$$cum(x_1, x_2, x_3) = E \{ x_1 x_2 x_3 \} \quad (3.2)$$

$$cum(x_1, x_2, x_3, x_4) = E \{ x_1 x_2 x_3 x_4 \} - E \{ x_1 x_2 \} E \{ x_3 x_4 \} -$$

$$E \{ x_1 x_3 \} E \{ x_2 x_4 \} - E \{ x_1 x_4 \} E \{ x_2 x_3 \}$$

There are several ways of collecting these random variables. In array processing, we collect samples of delayed sensor outputs; in system identification, we collect samples from a random process. In the system identification context, if  $x(t)$  is a random process, stationary up to order  $n$ , then the  $n$ th-order cumulant of  $x(t)$ ,  $C_{n,x}(\tau_1, \tau_2, \dots, \tau_{n-1})$ , is defined as the  $n$ th-order cumulant

of the random variables  $\{x(t), x(t + \tau_1), \dots, x(t + \tau_{n-1})\}$ , i.e.,

$$C_{n,x}(\tau_1, \tau_2, \dots, \tau_{n-1}) = \text{cum}(x(t), x(t + \tau_1), \dots, x(t + \tau_{n-1})) \quad (3.3)$$

Due to the stationarity assumption, the  $n$ th-order cumulant of the random process  $x(t)$  has  $(n - 1)$  degrees of freedom  $\{\tau_1, \tau_2, \dots, \tau_{n-1}\}$ . Since the  $n$ th-order cumulant can be expressed as a sum of joint moments of the random variables of orders up to  $n$ , its existence is established if all absolute moments of orders  $m \leq n$  exist and are bounded.

Note that for zero-mean processes the second- and third-order cumulants are identical to covariance and third-moment respectively. The third- and higher-order cumulants of Gaussian processes are identically zero. This fact can be used for detection and characterization of deviations from non-Gaussianity [56].

The following properties of cumulants are used frequently in applications [55]:

- [CP1] If  $\{\alpha_i\}_{i=1}^n$  are constants and  $\{x_i\}_{i=1}^n$  are random variables, then

$$\text{cum}(\alpha_1 x_1, \alpha_2 x_2, \dots, \alpha_n x_n) = \left( \prod_{i=1}^n \alpha_i \right) \text{cum}(x_1, x_2, \dots, x_n) \quad (3.4)$$

- [CP2] Cumulants are additive in their arguments,

$$\text{cum}(x_1 + y_1, x_2, \dots, x_n) = \text{cum}(x_1, x_2, \dots, x_n) + \text{cum}(y_1, x_2, \dots, x_n) \quad (3.5)$$

- [CP3] If the random variables  $\{x_i\}_{i=1}^n$  are independent of the random variables  $\{y_i\}_{i=1}^n$ , then

$$\text{cum}(x_1 + y_1, x_2 + y_2, \dots, x_n + y_n) = \text{cum}(x_1, x_2, \dots, x_n) + \text{cum}(y_1, y_2, \dots, y_n) \quad (3.6)$$

- [CP4] Cumulants suppress Gaussian noise of arbitrary covariance, i.e., if  $\{z_i\}_{i=1}^n$  are Gaussian random variables independent of  $\{x_i\}_{i=1}^n$  and  $n > 2$ , we have

$$\text{cum}(x_1 + z_1, x_2 + z_2, \dots, x_n + z_n) = \text{cum}(x_1, x_2, \dots, x_n) \quad (3.7)$$

- [CP5] If a subset of random variables  $\{x_i\}_{i=1}^n$  are independent of the rest, then

$$\text{cum}(x_1, x_2, \dots, x_n) = 0 \quad (3.8)$$

- [CP6] If  $\alpha_o$  is a constant, then

$$\text{cum}(\alpha_o + x_1, x_2, \dots, x_n) = \text{cum}(x_1, x_2, \dots, x_n) \quad (3.9)$$

Cumulants are blind to phase shifts and scale factors. This originates from their definition. Third-order cumulants are blind to processes that have a symmetric probability density function; consequently, fourth-order cumulants must be used in such environments. Cumulants of independent and identically distributed (i.i.d.) random processes are delta functions. i.e., if  $x(t)$  is such a process, then

$$C_{n,x}(\tau_1, \tau_2, \dots, \tau_{n-1}) = \gamma_{n,x} \delta_{\tau_1, \tau_2, \dots, \tau_{n-1}} \quad (3.10)$$

where  $\gamma_{n,x}$  is the  $n$ th-order cumulant of a single time sample from  $x(t)$ . It is important to note that joint moments do not possess this property. Furthermore, cumulants of order higher than two are blind to Gaussian noise and can reveal phase characteristics of the system under consideration. On the other hand, covariance-based approaches are blind to phase information and sensitive to

Gaussian noise. These properties, as proved in [57], make higher-order statistics candidates to previously unsolvable signal processing and communication problems.

In applications, we do not have access to true cumulants; we estimate them from the received data. The presence of additive Gaussian noise does effect the quality of the estimates, due to finite sample averaging in the estimation procedure. In order to get satisfactory results, longer data lengths are required for higher-order processing. An analysis of the asymptotical behavior of estimates of higher-order statistics can be found in [58].

### 3.2 Estimation of desired signal steering vector

In this section, we employ cumulants of received signals, to estimate the steering vector of the desired signal up to a constant factor. As described in Section 3.1, third-order cumulants are blind to signals with symmetric probability density function. On the other hand, most signals in communication environments have symmetric density functions, which motivates the use of fourth-order cumulants<sup>1</sup>. First, we define the *fourth-order zero-lag cumulant* operator of complex processes  $\{x_1(t), x_2(t), x_3(t), x_4(t)\}$ , based on (3.2), as

$$\begin{aligned} cum \{x_1(t), x_2(t), x_3(t), x_4(t)\} &\triangleq E \{x_1(t)x_2(t)x_3(t)x_4(t)\} - E \{x_1(t)x_2(t)\} E \{x_3(t)x_4(t)\} \\ &\quad - E \{x_1(t)x_3(t)\} E \{x_2(t)x_4(t)\} - E \{x_1(t)x_4(t)\} E \{x_2(t)x_3(t)\} \end{aligned} \quad (3.11)$$

Next, consider the vector  $\mathbf{c} = [c_1, c_2, \dots, c_M]^T$ , defined as

$$c_l \triangleq cum\{r_1(t), r_1^H(t), r_1^H(t), r_l(t)\} \quad l = 1, 2, \dots, M. \quad (3.12)$$

---

<sup>1</sup>An estimation procedure based on third-order statistics is presented in Appendix A.

As suggested in [55], there are various ways of defining fourth-order statistics of complex random processes. We follow the approach presented in [59] in (3.12). Since interference signals are independent of the desired signal and they are Gaussian with zero fourth-order cumulants ([CP4]), using (2.1) in (3.12) we can express  $c_l$  as

$$c_l = \text{cum} \{ a_1(\theta_d)d(t), a_1^H(\theta_d)d^H(t), a_1^H(\theta_d)d^H(t), a_1(\theta_d)d(t) \} \quad (3.13)$$

Using [CP1], we obtain

$$c_l = |a_1(\theta_d)|^2 a_1^H(\theta_d) \gamma_{d,4} a_l(\theta_d) \quad (3.14)$$

where  $\gamma_{d,4}$  denotes the *zeroth* lag of the *fourth-order* cumulant of the desired signal. Defining  $\beta_2 = |a_1(\theta_d)|^2 a_1^H(\theta_d) \gamma_{d,4}$  we have the following expression for the  $M \times 1$  vector  $\mathbf{c}$ :

$$\mathbf{c} = \beta_2 \mathbf{a}(\theta_d) \quad (3.15)$$

Observe that the vector  $\mathbf{c}$  is a *replica of the steering vector of the desired signal up to a scale factor*.

We show in the next section how this information can be used to recover the desired signal.

### 3.3 Interference Rejection

With the knowledge of the steering vector of the desired signal, interference rejection is possible using the following minimum-variance distortionless response formulation: find the weight vector  $\mathbf{w}$  that minimizes the power,  $\mathbf{w}^H \mathbf{R} \mathbf{w}$ , at the output of the beamformer subject to the constraint  $\mathbf{w}^H \mathbf{c} = 1$ , where  $\mathbf{c}$  is obtained via the cumulant-based estimation procedure described in Sec-



tion 3.2. The solution to this optimization problem is well-known [10], and can be expressed as

$$\mathbf{w}_{cum} = \beta_3 \mathbf{R}^{-1} \mathbf{c} \quad (3.16)$$

where the constant  $\beta_3 = (\mathbf{c}^H \mathbf{R}^{-1} \mathbf{c})^{-1}$  is present in order to maintain the linear constraint.

Due to the constraint  $\mathbf{w}^H \mathbf{c} = 1$ , the power minimization procedure does not cancel the desired signal, but rejects all interference components and sensor noise in the best possible manner. Note that this is accomplished without knowledge of covariance structure of interference signals, sensor noise or array manifold. In the sequel, we refer to the processor in (3.16) as CUM<sub>1</sub>. The proof that this cumulant-based beamformer is identical to the maximum SINR processor is provided in Chapter 5, where the general multipath case is treated.

## Chapter 4

# Robust Beamforming

In this chapter, we first propose an approach that utilizes the received data in the estimation of the source steering vector in a more efficient manner. We then suggest a method that uses both cumulants and covariance information under some scenarios. Finally, we employ a robust method to combat the effects of estimation errors.

### 4.1 Efficient Utilization of Array Data

In the previous chapter, we presented a method of blind estimation of the desired source steering vector from the received data; however, the proposed approach is rather inefficient in the sense that only the first sensor is taken as reference. For example, if the connection from this element to the processor is broken, then the estimation objective can not be accomplished. Similarly, due to poor receiving circuitry following this array element, the reference signal may be very noisy, degrading the quality of the estimate. We can overcome these difficulties by using multiple reference elements.

Define the matrix  $\mathbf{C}$  with the  $(k, l)$ th element,

$$C_{k,l} \triangleq \text{cum}\{r_k(t), r_k^H(t), r_k^H(t), r_l(t)\} \quad \text{where } k, l = 1, \dots, M. \quad (4.1)$$

With true statistics, the cross-cumulant matrix  $\mathbf{C}$  will have rank 1, since all its columns are scaled replicas of the desired source steering vector; however, with sample statistics this condition never holds. The left singular vector of  $\mathbf{C}$  with the largest singular value can be used as the estimate of the desired source steering vector removing the effects of noise. In this way, we utilize array data more efficiently<sup>1</sup>. The beamformer that employs the steering vector estimate obtained in the way described above is referred to as the CUM<sub>2</sub> beamformer in the sequel.

In addition, the Total Least Squares algorithm, that takes the errors in both the received data covariance matrix estimate and the steering vector estimate into account, is a better choice for computing the optimum weight vector, as suggested in [52], but it is computationally expensive. If extra computations are feasible, we suggest the use of the Constrained Total Least Squares algorithm [60], for even better numerical results.

## 4.2 Covariance-Cumulant ( $\mathbf{C}^2$ ) Approach

In some array processing applications, sensor noise covariance structure has a definite structure enabling a whitening operation on the received data. The principal eigenvectors of the covariance matrix of this processed data reveal the subspace spanned by the steering vectors of directional signals illuminating the array [17]. Hence, the steering vector estimate obtained by the cumulant-based approach can be improved by projecting this estimate on the subspace spanned by the

---

<sup>1</sup>A method that utilizes the array data even more efficiently is presented in Appendix B.

principal eigenvectors of the covariance matrix. This improved estimate can then be used in the beamforming procedure of Section 3.3. The motivation behind this approach is that covariance estimates exhibit less variance than cumulant estimates, but in the covariance domain we can not identify the source steering vector if there are multiple sources. This procedure yields an estimate of the steering vector from covariance-matrix information by employing the cumulant-based estimate as side information. A mathematical description of this approach is presented below:

1. From the received data, estimate the covariance matrix  $\mathbf{R}$  and the desired signal steering vector  $\mathbf{c}$  by the cumulant-based procedure.
2. Perform an eigendecomposition of the sample covariance matrix, to reveal the signal and noise subspaces: the eigenvectors of  $\mathbf{R}$  with the repeated minimum eigenvalue span the noise subspace [17], while the rest span the signal subspace.
3. Assume the signal subspace is  $(J + 1)$  dimensional. Then, the basis vectors for the signal subspace, obtained from the eigendecomposition procedure, can be sorted in an  $M \times (J + 1)$  matrix  $\mathbf{E}_s$  with the column space identical to the signal subspace.
4. Project the cumulant-based steering vector estimate  $\mathbf{c}$ , on the signal subspace to obtain an improved estimate  $\mathbf{c}_{imp}$ , as

$$\mathbf{c}_{imp} = \mathbf{E}_s \mathbf{E}_s^H \mathbf{c}$$

5. Compute the weights for the beamformer, as

$$\mathbf{w}_{imp} = \mathbf{R}^{-1} \mathbf{c}_{imp}$$

### 4.3 Robustness Constraint

Any estimation procedure is inevitably subject to errors. MVDR beamforming is extremely sensitive to mismatch [24]-[30], especially in high SNR conditions and in arrays with large number of elements. A variety of constraints have been summarized in [6] assuming perfect knowledge of element characteristics and locations; however, in our case these methods are not applicable since there is no available information about the array manifold to design effective constraints.

Errors in the steering vector estimate result in signal cancellation. This mismatch condition, arising from non-perfect estimation, can be viewed as the problem of optimum beamforming with an array of sensors at slightly perturbed locations. In [35], a method that constrains the white noise gain of the processor is proposed for the solution of the latter problem. In this section, we use the same approach to alleviate the effects of estimation errors in cumulant-based optimum beamforming.

In order to understand the mismatch problem and find a way to alleviate its effects, we need to analyze the problem analytically. Consider the power response of a beamformer with a weight vector  $\mathbf{w}$ , as a function of DOA  $\theta$ , defined as

$$P(\theta) \triangleq |\mathbf{w}^H \mathbf{a}(\theta)|^2 \quad (4.2)$$

with  $\mathbf{a}(\theta)$  denoting the steering vector for an arrival from  $\theta$ . The derivative,  $\partial P(\theta)/\partial\theta$ , can be expressed, as

$$\frac{\partial P(\theta)}{\partial\theta} = 2\text{Re}\{ \mathbf{w}^H \mathbf{a}(\theta) [ \sum_{l=1}^M w_l \frac{\partial}{\partial\theta} a_l^H(\theta) ] \} \quad (4.3)$$

Now consider the following scenario: we have an MVDR processor *looking* at  $\theta_o$ , which is the

expected DOA for the desired signal. Instead, the source illuminates the array from  $\theta_d$  which is very close but not equal to  $\theta_o$ . In this case, the beamformer treats the desired signal as interference and nulls it; however, due to the distortionless response constraint for  $\theta_o$ , and since the angles are very close, the derivative  $\partial P(\theta)/\partial\theta$  must be large in magnitude for  $\theta$  between  $\theta_d$  and  $\theta_o$ . From the derivative expression (4.3), it is clear that this is possible only if the norm of the weight vector increases, since the inner product,  $\mathbf{w}^H \mathbf{a}(\theta)$ , and, the derivatives,  $\{\frac{\partial}{\partial\theta} a_i^H(\theta)\}_{i=1}^M$  are bounded. In this situation, the constraint is maintained by increasing the angle between the weight vector and the look-direction steering vector. This phenomena was exploited in [34], for tuning the beamformer to acquire a weak desired signal in the presence of strong interference.

Note that the white-noise amplification factor for any processor with a weight vector  $\mathbf{w}$  is  $\mathbf{w}^H \mathbf{w}$ ; hence, the nulling phenomena can be prevented if the white noise level at the processor is sufficiently high so that output power minimization criterion limits the increase in the norm of  $\mathbf{w}$ . This can be achieved by perturbing the covariance matrix estimate of array measurements by a scaled identity matrix as,

$$\mathbf{R}_p = \mathbf{R} + \epsilon \mathbf{I} \quad (4.4)$$

where  $\epsilon$  is a non-negative parameter which adjusts the strength of perturbation. Alternatively, it is possible to coin a term *virtual* SNR,  $\text{SNR}_v$ , defined as

$$\text{SNR}_v = \text{SNR} - 10 \log_{10} \left( \frac{\epsilon + \sigma_n^2}{\sigma_n^2} \right) \quad (4.5)$$

We then determine the weight vector as,

$$\mathbf{w} = \mathbf{R}_p^{-1} \mathbf{a}(\theta_o) \quad (4.6)$$

A recent method presented in [35] performs this procedure in an adaptive fashion by a simple scaling of the weight vector. In our case, we do not have source DOA information, but we do have an estimate of the steering vector. It is therefore possible to use this estimate in place of  $\mathbf{a}(\theta_o)$  in (4.6) to formulate the cumulant-based processor with limited signal nulling property.

## Chapter 5

# Multipath Phenomena

Eigendecomposition-based high-resolution methods [11]-[21] have proven to be effective means of obtaining bearing estimates of far-field narrowband sources from noisy measurements. The performance of these algorithms is severely degraded when coherence is present. Several methods have been proposed to solve the coherent signals problem with restrictions on array geometry [44]-[50]; however, with lack of knowledge of array manifold it is not possible to solve the coherence problem. MVDR beamforming also fails to perform optimally, when interference signals are correlated with the desired signal [51]-[52]. In some scenarios, even the conventional beamformer outperforms the MVDR approach due to signal cancellation in the MVDR beamformer.

In Chapter 3, we showed that the cumulant-based beamformer is not affected by the presence of coherence among interfering Gaussian signals as long as they are not correlated with the desired signal. The same is not possible for high-resolution DOA estimation methods; but, the MVDR beamformer may perform equally well if the desired signal steering vector is known and a satisfactory estimate of  $\mathbf{R}$  is available. In this chapter, we show that the cumulant-based approach is not affected by the presence of multipath propagation of the desired signal. In addition, we show that



the cumulant-based processor turns out to be the maximal-ratio-combiner [61] that maximizes the SINR.

With the presence of multipath propagation or smart jamming, our signal model in (2.1) changes to

$$r_k(t) = d(t) \sum_{l=1}^L a_k(\theta_{d_l}) \eta_l + \sum_{j=1}^J a_k(\theta_{i_j}) i_j(t) + n_k(t) \quad (5.1)$$

or in vector form

$$\mathbf{r}(t) = \begin{bmatrix} \mathbf{a}(\theta_{d_1}), \mathbf{a}(\theta_{d_2}), \dots, \mathbf{a}(\theta_{d_L}) \end{bmatrix} \begin{bmatrix} \eta_1 \\ \eta_2 \\ \vdots \\ \eta_L \end{bmatrix} d(t) + \mathbf{A}_I \mathbf{i}(t) + \mathbf{n}(t) \quad (5.2)$$

where the set of scalars  $\{ \eta_1, \eta_2, \dots, \eta_L \}$  constitute the multipath coefficients for an  $L$ -ray scenario.

The set of vectors,  $\{ \mathbf{a}(\theta_{d_1}), \mathbf{a}(\theta_{d_2}), \dots, \mathbf{a}(\theta_{d_L}) \}$  are the corresponding steering vectors of the  $L$ -ray model. Letting

$$\mathbf{b} \triangleq \begin{bmatrix} \mathbf{a}(\theta_{d_1}), \mathbf{a}(\theta_{d_2}), \dots, \mathbf{a}(\theta_{d_L}) \end{bmatrix} \begin{bmatrix} \eta_1 \\ \eta_2 \\ \vdots \\ \eta_L \end{bmatrix} = \mathbf{A}_D \boldsymbol{\eta} \quad (5.3)$$

we can reduce the signal model for multipath phenomena to the single-ray propagation model of Section 2.1,

$$\mathbf{r}(t) = \mathbf{b} d(t) + \mathbf{A}_I \mathbf{i}(t) + \mathbf{n}(t) \quad (5.4)$$

because we can view the vector  $\mathbf{b}$  as a *generalized* steering vector for a single desired signal although it may not be a vector in the array manifold. Therefore, following our work in Chapter 3, cumulant-based blind estimation procedure will yield

$$\mathbf{c} = \beta_4 \mathbf{b} \quad (5.5)$$

where  $\beta_4 = |b_1|^2 b_1^H \gamma_{d,4}$ , in which  $b_1$  is the first component of  $\mathbf{b}$ . Incorporating (5.5) into the constrained power minimization procedure, we obtain the following weight vector,

$$\mathbf{w}_{cum} = \beta_5 \mathbf{R}^{-1} \mathbf{c} = \beta_4 \beta_5 \mathbf{R}^{-1} \mathbf{b} \quad (5.6)$$

where  $\beta_5 = (\mathbf{c}^H \mathbf{R}^{-1} \mathbf{c})^{-1}$ .

Next, we find an alternate expression for  $\mathbf{w}_{cum}$ . Recall that the optimization problem which results in  $\mathbf{w}_{cum}$  is: minimize  $\mathbf{w}^H \mathbf{R} \mathbf{w}$  subject to  $\mathbf{w}^H \mathbf{c} = 1$ , or by (5.5),  $\mathbf{w}^H \mathbf{b} = 1/\beta_4$ . We can express the output power in the following way by using (2.9) and (5.4),

$$\mathbf{w}^H \mathbf{R} \mathbf{w} = \sigma_d^2 |\mathbf{w}^H \mathbf{b}|^2 + \mathbf{w}^H \mathbf{R}_u \mathbf{w} \quad (5.7)$$

but, due to the constraint  $\mathbf{w}^H \mathbf{b} = 1/\beta_4$ , the first term in the above expression is a constant. Therefore, the original optimization problem can be translated into : minimize  $\mathbf{w}^H \mathbf{R}_u \mathbf{w}$ , subject to  $\mathbf{w}^H \mathbf{c} = 1$  or equivalently,  $\mathbf{w}^H \mathbf{b} = 1/\beta_4$ . The solution to this problem is

$$\mathbf{w}_{cum} = \beta_6 \mathbf{R}_u^{-1} \mathbf{c} \quad (5.8)$$

where  $\beta_6 = (\mathbf{c}^H \mathbf{R}^{-1} \mathbf{c})^{-1}$ . Of course, this solution can also be expressed in terms of  $\mathbf{b}$ , as

$$\mathbf{w}_{cum} = \beta_7 \mathbf{R}_u^{-1} \mathbf{b} \quad (5.9)$$

where  $\beta_7 = \beta_4 \beta_6$ .

Note that although (5.8) and (5.9) are alternate expressions for  $\mathbf{w}_{cum}$ , they are not the way to actually compute  $\mathbf{w}_{cum}$ , since  $\mathbf{R}_u$  is not available in general.

Next, we determine the weight vector that yields the maximum SINR. SINR can be expressed as a function of the weight vector of the beamformer, as

$$\text{SINR}(\mathbf{w}) = \sigma_d^2 \frac{\mathbf{w}^H \mathbf{b} \mathbf{b}^H \mathbf{w}}{\mathbf{w}^H \mathbf{R}_u \mathbf{w}} \quad (5.10)$$

Defining,  $\mathbf{v} = \mathbf{R}_u^{1/2} \mathbf{w}$  so that  $\mathbf{w} = \mathbf{R}_u^{-1/2} \mathbf{v}$ , we can reexpress (5.10), as

$$\text{SINR}(\mathbf{w}) = \text{SINR}(\mathbf{R}_u^{-1/2} \mathbf{v}) = \sigma_d^2 \frac{|\mathbf{v}^H \mathbf{R}_u^{1/2} \mathbf{b}|^2}{\mathbf{v}^H \mathbf{v}} \quad (5.11)$$

Applying the Schwarz inequality [50] to (5.11), we find that

$$\text{SINR}(\mathbf{w}) = \text{SINR}(\mathbf{R}_u^{-1/2} \mathbf{v}) \leq \sigma_d^2 \|\mathbf{R}_u^{-1/2} \mathbf{b}\|^2 = \sigma_d^2 \mathbf{b}^H \mathbf{R}_u^{-1} \mathbf{b} \quad (5.12)$$

where equality holds if and only if

$$\mathbf{v} = \beta_8 \mathbf{R}_u^{-1/2} \mathbf{b} \quad (5.13)$$

in which  $\beta_8$  is a non-zero constant. Consequently, the optimum weight vector  $\mathbf{w}_{\text{SINR}}$ , which yields

the maximum SINR, can be determined from  $\mathbf{w} = \mathbf{R}_u^{-1/2} \mathbf{v}$  and (5.13), as

$$\mathbf{w}_{\text{SINR}} = \beta_8 \mathbf{R}_u^{-1} \mathbf{b} \quad (5.14)$$

Based on this derivation, some comments are in order. It is clear, by comparing (5.9) and (5.14), that the cumulant-based beamformer does indeed yield the maximum possible SINR, since  $\mathbf{w}_{cum}$  is just a scaled version of  $\mathbf{w}_{\text{SINR}}$ . This observation proves that the cumulant-based beamformer is optimal. In addition,  $\mathbf{w}_{cum}$  can be computed from the received data, whereas  $\mathbf{w}_{\text{SINR}}$ , as implemented in (5.14), requires knowledge of  $\mathbf{R}_u$ , which can not be determined from the received data in the presence of the desired signal. Finally, note that robust approaches presented in Chapter 4 are directly applicable in the presence of multipath.

## Chapter 6

# Adaptive Processing

In real-world applications, adaptive beamforming is an important requirement, especially when the desired signal source is in relative motion with respect to the array. In this chapter, we address this problem by providing an “estimate and plug” type of adaptive algorithm for the CUM<sub>1</sub> method.

The beamforming procedure (3.16) requires the inverse of the sample covariance matrix to compute the weights. We can estimate the covariance matrix recursively, as

$$\hat{\mathbf{R}}_t = (1 - \alpha_1)\hat{\mathbf{R}}_{t-1} + \alpha_1 \mathbf{r}(t)\mathbf{r}^H(t) \quad (6.1)$$

Since we need to propagate the inverse of  $\hat{\mathbf{R}}_t$ , we use the Sherman-Morrison formula [62], to obtain

$$\hat{\mathbf{R}}_t^{-1} = \frac{1}{1 - \alpha_1} \left[ \hat{\mathbf{R}}_{t-1}^{-1} - \alpha_1 \frac{\hat{\mathbf{R}}_{t-1}^{-1} \mathbf{r}(t) \mathbf{r}^H(t) \hat{\mathbf{R}}_{t-1}^{-1}}{1 - \alpha_1 [1 - \mathbf{r}^H(t) \hat{\mathbf{R}}_{t-1}^{-1} \mathbf{r}(t)]} \right] \quad t = 1, 2, \dots \quad (6.2)$$

with  $\hat{\mathbf{R}}_0^{-1} = \gamma \mathbf{I}$  where  $\gamma$  is a large positive number and  $\alpha_1$  controls the learning rate for second-order statistics.

To compute the weight vector, we also need the cumulant-based estimate of the source steering vector  $\mathbf{c}$ . We can estimate it recursively as

$$\hat{c}_l(t) = (1 - \alpha_2)\hat{c}_l(t-1) + \alpha_2[|r_1(t)|^2 r_1^H(t)r_l(t) - 2p(t)q(t) - v^H(t)x(t)] \quad (6.3)$$

with the auxiliary processes defined as

$$p(t) = (1 - \alpha_3)p(t-1) + \alpha_3|r_1(t)|^2$$

$$q(t) = (1 - \alpha_3)q(t-1) + \alpha_3 r_1^H(t)r_l(t)$$

$$v(t) = (1 - \alpha_3)v(t-1) + \alpha_3 r_1^2(t)$$

$$x(t) = (1 - \alpha_3)x(t-1) + \alpha_3 r_1(t)r_l(t)$$

The auxiliary processes are required in order to implement the cross-correlation terms in (3.11). The initial values for the auxiliary processes can be set to zero. Different learning rates are provided to emphasize the fact that higher-order statistics require longer periods to acquire the required information.

We can perform adaptive beamforming by computing the weight vector at each time as

$$\mathbf{w}(t) = \hat{\mathbf{R}}_t^{-1} \hat{\mathbf{c}}(t) \quad (6.4)$$

and obtain the array output, as

$$y(t) = \mathbf{w}^H(t)\mathbf{r}(t). \quad (6.5)$$

Adaptive versions of  $CUM_2$  and  $C^2$  methods will appear in a later publication.

## Chapter 7

# Simulations

In this chapter we present various experiments to illustrate the performance of cumulant-based beamforming. In all of the experiments we employed a uniformly spaced linear array, rather than an arbitrary geometry. This is done for two reasons: covariance-based techniques are mainly designed for this type of array structure, e.g., the spatial smoothing algorithm [44]- [50], so that it will be possible to compare both previous and future work with our current results. In addition, allowing a sufficient number of multipath rays, it is possible to represent any arbitrary steering vector by the linear array, since the steering vectors of the uniformly spaced isotropic linear array exhibit Vandermonde structure, resulting in linearly independent vectors for different DOA's. In all batch type of experiments, the record length is 1000 snapshots and the array has 10 isotropic elements with uniform half-wavelength spacing.



## 7.1 Experiment 1: Desired Signal in White-Noise

In this experiment, we employ the linear array described above for optimum reception of a BPSK signal, which is expected to arrive from broadside in the presence of temporally and spatially white, equal power, circularly symmetric sensor noise; however, the desired source illuminates the array from  $5^\circ$  broadside.

Our first MVDR beamformer,  $MVDR_1$ , looks to broadside, i.e., a mismatch condition. Our second MVDR beamformer,  $MVDR_2$ , uses exact knowledge of DOA of the desired signal. We also employ the cumulant-based beamformer of Chapter 3,  $CUM_1$ , and the improved cumulant-based beamformer  $CUM_2$  of Section 4.1. We investigate the performance of these processors for the following two elemental SNR levels: 20 dB for a strong signal and 0 dB for a weak signal. Note that the white-noise gain of any processor is limited to 10 dB by the number of sensors [35].

The beampattern responses (4.2), and white-noise gains of these beamformers are presented in Figure 7.1 for SNR=20 dB. All responses are normalized to have a maximum value of 0 dB. For comparison purposes, the optimum beamformer response, calculated by using true statistics in (3.16), is presented as the dashed curves. Observe that due to the mismatch condition,  $MVDR_1$  nulls the desired signal. More interestingly, the  $MVDR_2$  processor that utilizes the true DOA information does not improve the SNR, due to the mismatch arising from the use of a sample-data covariance matrix. The cumulant-based processors,  $CUM_1$  and  $CUM_2$ , yield excellent performance without any knowledge of source DOA. It is very important to observe that the performance of cumulant-based processors are better than that of the MVDR with exactly known look-direction.

We performed 100 Monte-Carlo runs to investigate the performance in a better way. The results are given in Table 7.1.

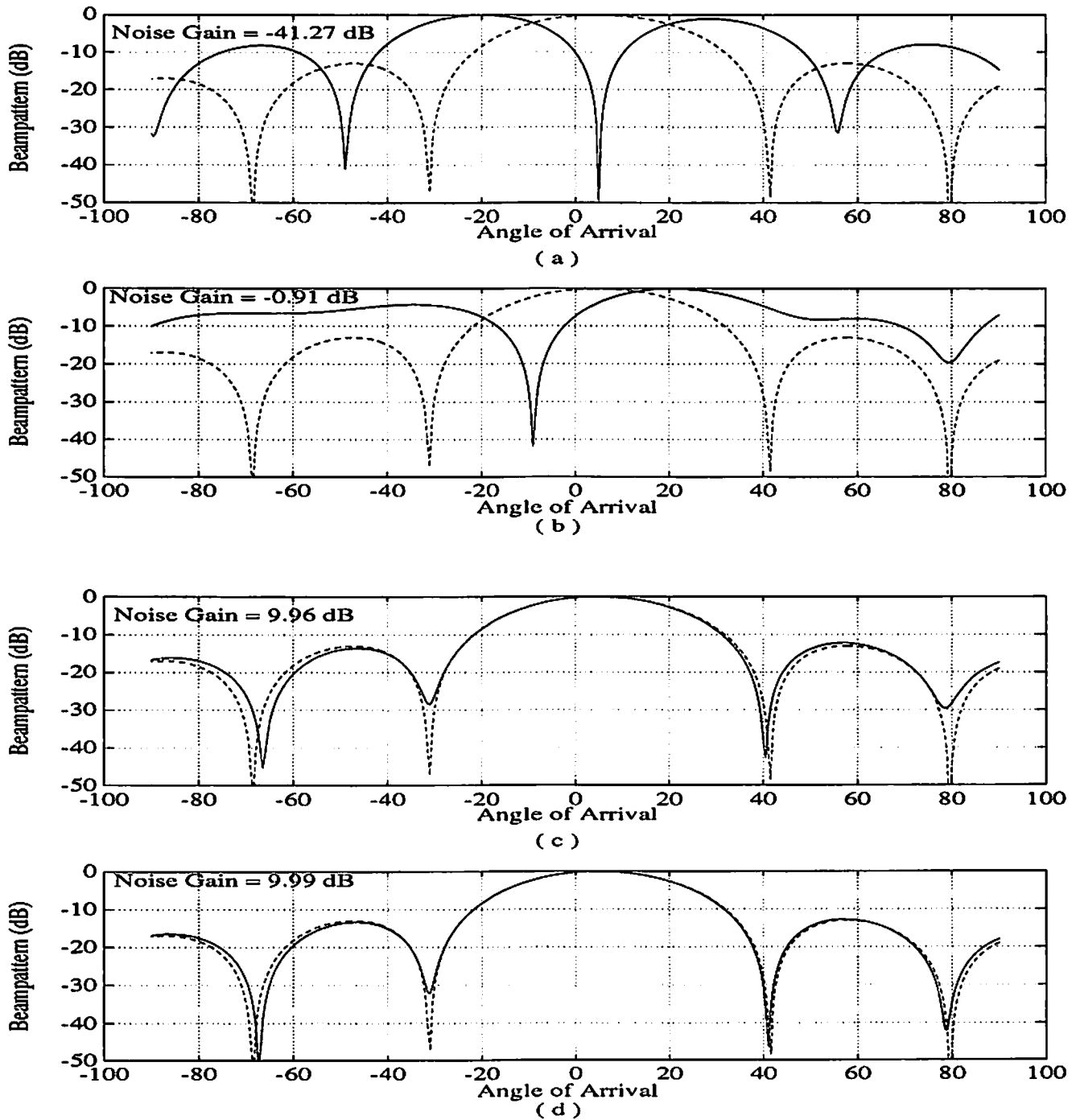


Figure 7.1: Beampatterns and white-noise gains of processors in a single realization for SNR = 20 dB : (a) MVDR<sub>1</sub>, (b) MVDR<sub>2</sub>, (c) CUM<sub>1</sub>, (d) CUM<sub>2</sub>. The optimum pattern is illustrated in dashed lines for comparison purposes.

Table 7.1: Results from 100 Monte-Carlo Runs for Experiment 1

Processor	White-Noise Gain (dB)			
	SNR=20dB		SNR=0dB	
	Mean	Std.	Mean	Std.
MVDR <sub>1</sub>	-38.130	1.579	0.413	0.281
MVDR <sub>2</sub>	0.179	1.360	9.583	0.131
CUM <sub>1</sub>	9.954	0.015	9.058	0.359
CUM <sub>2</sub>	9.990	0.003	9.959	0.014

From these results, it is clear that cumulant-based processors are superior and the extra computation involved in CUM<sub>2</sub> reduces the variations. Note, also, that variations in the MVDR processors are significantly larger than those of the cumulant-based counterparts. This agrees with the previous remarks about the sensitivity of MVDR processing to experimental conditions in a high-SNR environment.

We performed the same experiment for 0 dB SNR condition. Figure 7.2 illustrates the beam-pattern responses and white-noise gains of the processors. Monte-Carlo results are also given in Table 7.1. In this low-SNR condition, MVDR results are expected to improve since the mismatch conditions for the desired signal will be masked by the presence of white noise of comparable power, as explained in Chapter 4. MVDR<sub>1</sub> processor does not offer a significant gain due to the persistent mismatch condition, but MVDR<sub>2</sub> yields a near-optimum result, since presence of higher-level noise masks the mismatch due to the use of a sample-covariance matrix. The performance of CUM<sub>1</sub> processor is slightly below than that of MVDR<sub>2</sub> and exhibits more variations. This is due to the inefficient use of the array data, since a high-level of noise corrupts the cumulant estimates and with CUM<sub>1</sub> there are no precautions to combat these errors. As expected, CUM<sub>2</sub> overcomes this problem by using SVD. Results in Table 7.1 indicate that CUM<sub>2</sub> achieves the best performance

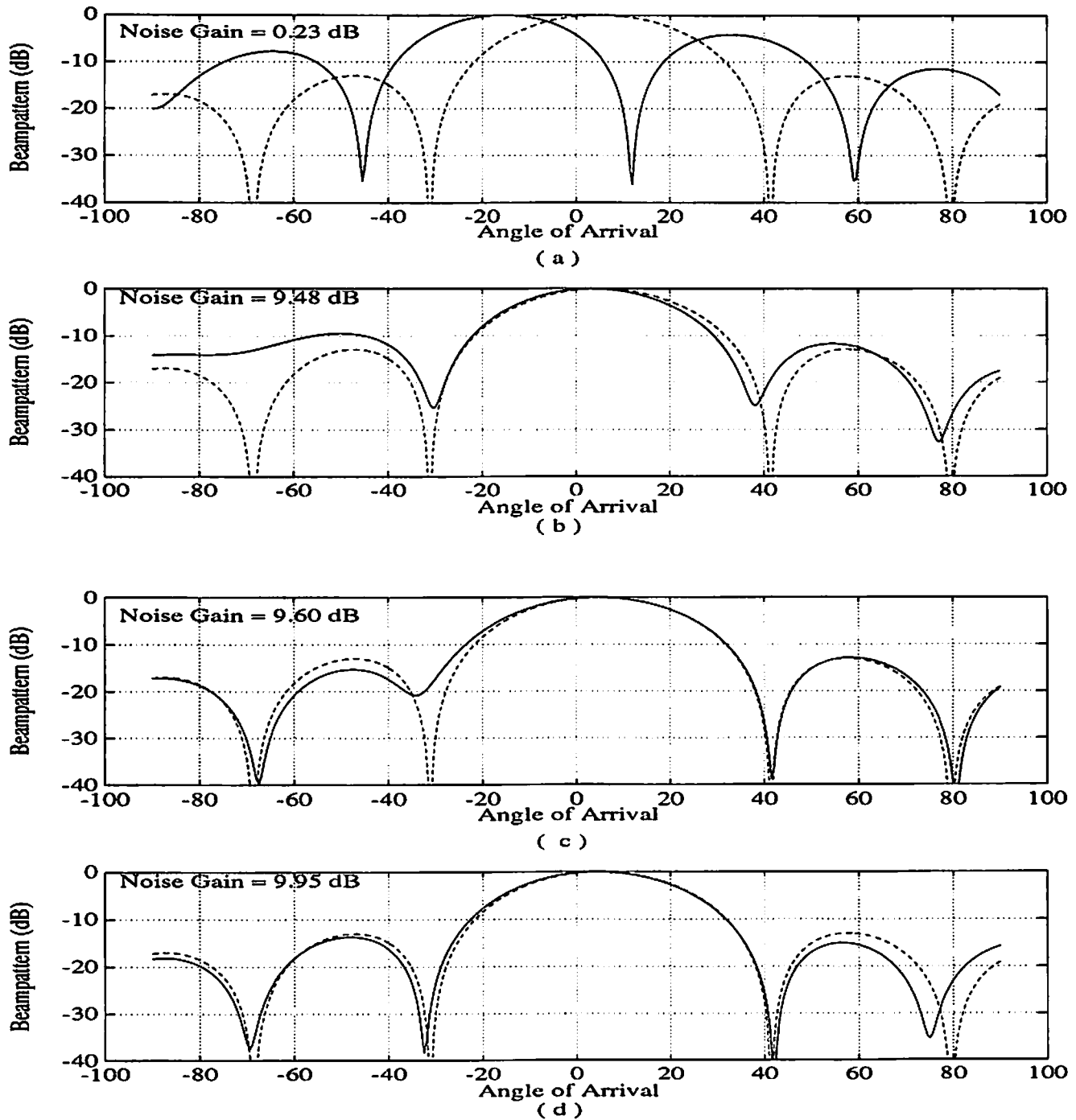


Figure 7.2: Beampatterns and white-noise gains of processors in a single realization for SNR = 0 dB : (a) MVDR<sub>1</sub>, (b) MVDR<sub>2</sub>, (c) CUM<sub>1</sub>, (d) CUM<sub>2</sub>. The optimum pattern is illustrated in dashed lines for comparison purposes.

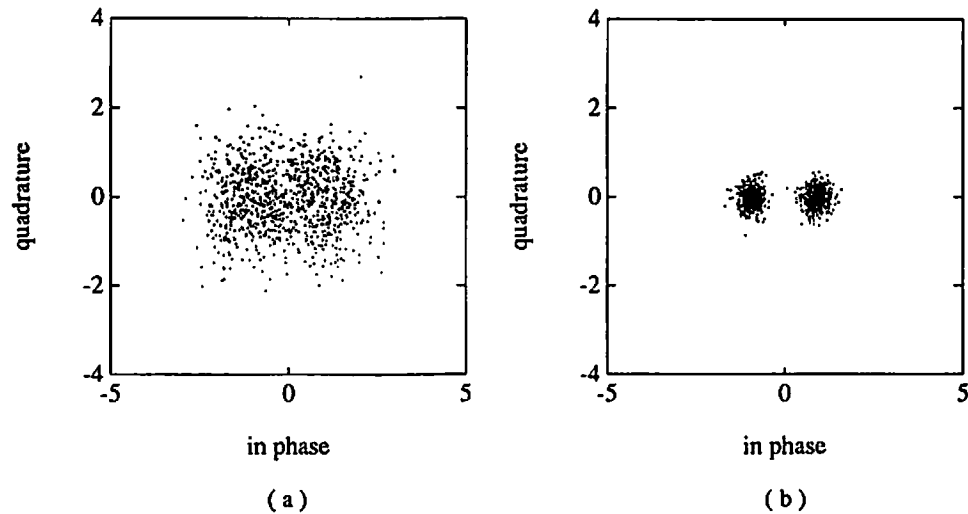


Figure 7.3: Power of cumulant-based beamforming: (a) received signal at the reference element at SNR = 0 dB, (b) output of CUM<sub>2</sub> processor.

with minimum variations.

Finally, to demonstrate the power of cumulant-based beamforming, we illustrate the received signal and the output of CUM<sub>2</sub> processor for SNR=0 dB case in Figure 7.3. It is clear that CUM<sub>2</sub> is capable of sufficient noise rejection for performing correct decisions.

## 7.2 Experiment 2: Spatially Colored Noise and Multipath Propagation

In this experiment, we investigate the performance of the proposed approach in the presence of spatially colored noise. We employ the linear array of the previous experiment. We assume that the

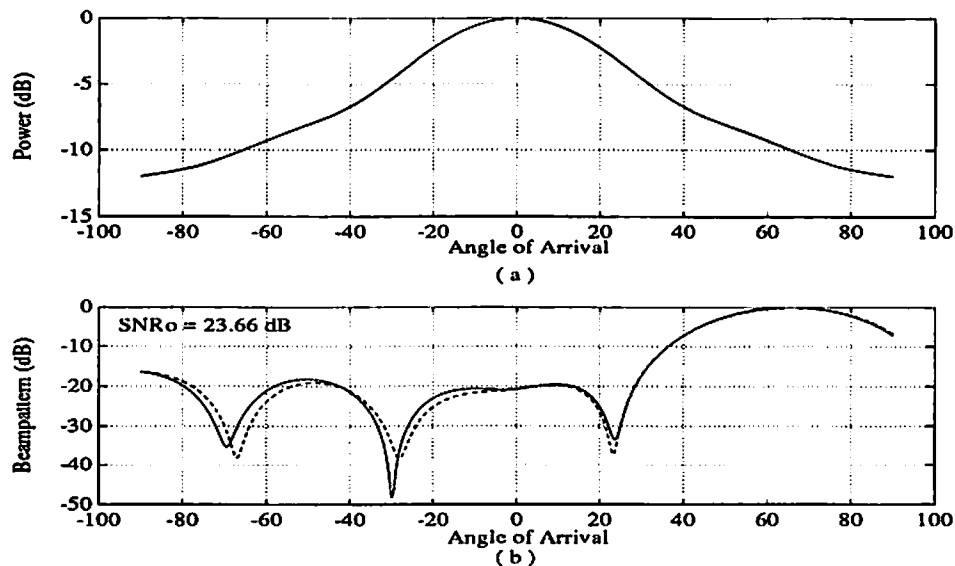


Figure 7.4: Beamforming in the presence of spatially colored noise: (a) Spatial Power Spectral Density of noise, (b) Beampattern of CUM<sub>2</sub> processor. The optimum pattern is illustrated in dashed lines for comparison purposes.

noise field is created by a set of point sources distributed symmetrically about the broadside of the linear array. As suggested in [63], this source structure is typical when the noise field is spherically or cylindrically isotropic. In this case, the noise covariance matrix is symmetric-Toeplitz. In our experiment, we use the following structure for the covariance matrix of undesired components,

$$\mathbf{R}_u(i, j) = 0.8^{|i-j|} \quad (7.1)$$

The spatial power spectrum of undesired components is illustrated in Figure 7.4a. It is clear that most of the noise leaks into the system from broadside. The desired signal illuminates the array from broadside, with an SNR of 10 dB. To illustrate the optimum combining property of our approach, we implanted an exact replica of the desired signal illuminating the array from 60°, where noise power is relatively less when compared to that from broadside. The beampattern of CUM<sub>2</sub>

Table 7.2: Results from 100 Monte-Carlo Runs for Experiment 2

Processor	SNR <sub>o</sub> (dB)	
	Mean	Std
CUM <sub>1</sub>	23.641	0.017
CUM <sub>2</sub>	23.645	0.015

processor is given in Figure 7.4b. For comparison purposes, we present the response of the optimum beamformer based on exact statistical information, as a dashed curve. The maximum-possible SNR at the output is 23.689 dB for this scenario. It is clear that the response of CUM<sub>2</sub> is almost identical to that of the optimum beamformer: both processors emphasize the signal illuminating the array from 60°, since the noise contribution is less in this region. We performed 100 Monte-Carlo runs for this scenario, and the results are presented in Table 7.2. It is clear that both cumulant-based processors perform equally well. The reason for this phenomenon is the presence of the multipath from 60° through a low-noise background that virtually increases the effective SNR, which, in turn, alleviates the effects of estimation errors. Note that the peak of the beampattern is slightly shifted from 60°, in order to receive less interference. Similar behavior is observed in covariance-based direction-of-arrival estimation in the presence of colored noise resulting in biased estimates of parameters.

### 7.3 Experiment 3: Effects of Robustness Constraint

In this experiment, we illustrate the effects of the robustness constraint of Section 4.3, on a CUM<sub>1</sub> processor in the presence of white noise. We employ the same array as in the previous experiments. We employ CUM<sub>1</sub>, since this processor uses the data inefficiently, and requires a robust approach. In our experiment, we consider the situation with SNR=0 dB. Figure 7.5 illustrates the beampatterns

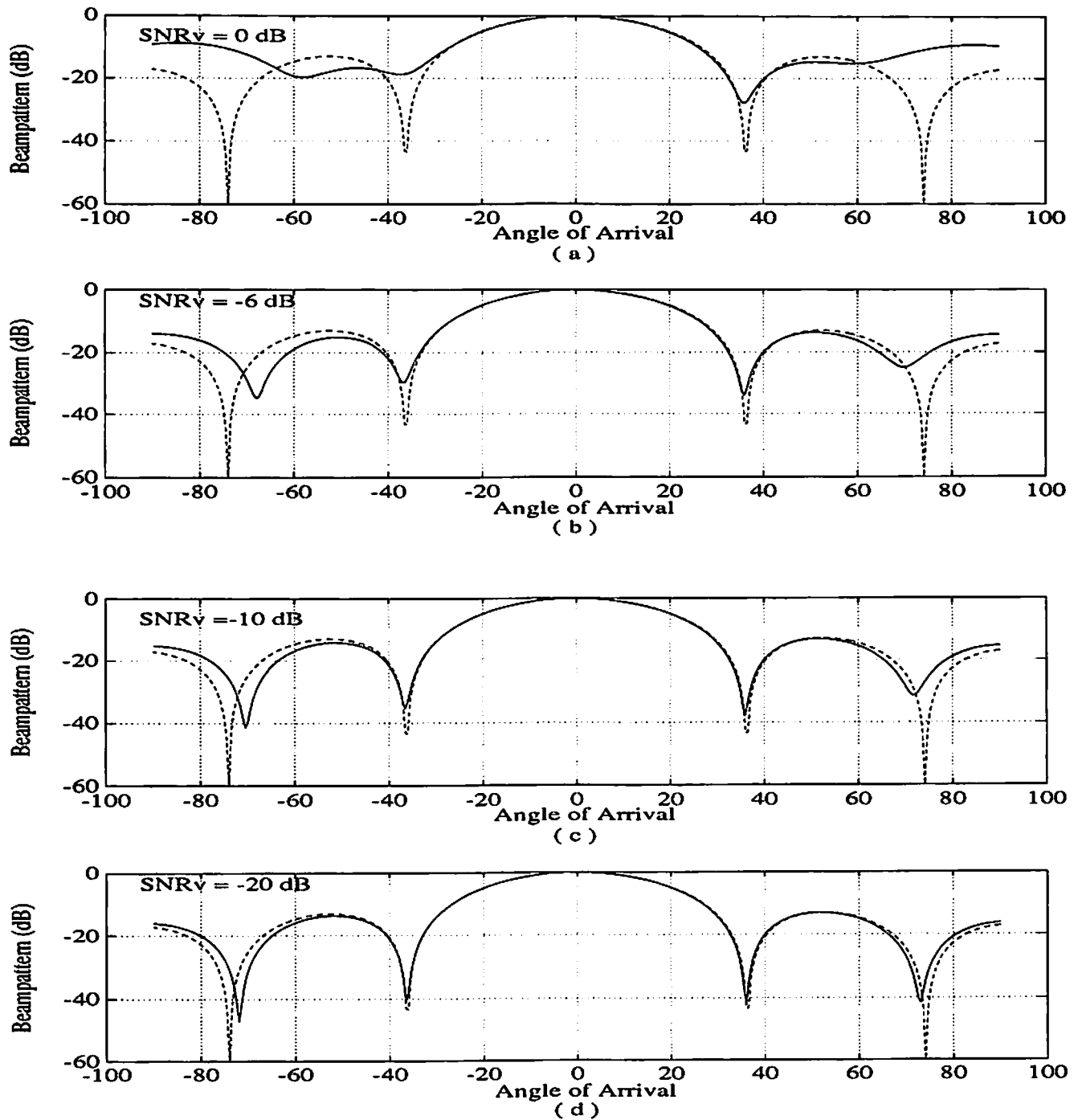


Figure 7.5: Beampattern of CUM<sub>1</sub> processor for varying virtual SNR: (a) 0 dB, (b) -6 dB, (c) -10 dB, (d) -20 dB. The optimum pattern is illustrated in dashed lines for comparison purposes.



of  $CUM_1$  processor for several  $SNR_p$  values. It is clear from the results that, as the perturbation increases, the patterns match better since the mismatch due to estimation errors in the steering vector estimate are masked by the presence of virtual increased level of noise. This method should be used sparingly in the presence of jammers, because increasing the virtual noise level results in diverting the capability of the array from nulling the directional interference.

## 7.4 Experiment 4: Multiple Interferers

In this experiment, we consider the problem of beamforming in a multipath environment in the presence of multiple jammers. We employ the same array as in the previous experiments. The signal of interest originates from a BPSK communication source, and it is expected from broadside; however, due to multipath effects, multiple delayed and shifted replicas are received. There are two jammers, and one is subject to multipath as well. Table 7.3 summarizes the signal structure. Note that there are 10 wavefronts illuminating the array and it is not possible to estimate their

Table 7.3: Signal structure for Experiment 4

Source	Power (dB)	Multipath Coeff.	DOA
BPSK	10	(0.0,-0.5)	$-10^\circ$
		(0.9895,-0.0311)	$-2^\circ$
		(1.0,0.0)	$0^\circ$
		(-0.6472,-0.4702)	$6^\circ$
		(-0.8,0.0)	$8^\circ$
		(0.1414,0.1414)	$11^\circ$
		(0.0462,0.0191)	$18^\circ$
JAMMER <sub>1</sub>	10	(1.0,0.0)	$26^\circ$
		(0.5657,0.5657)	$32^\circ$
JAMMER <sub>2</sub>	10	(1.0,0.0)	$-1^\circ$
NOISE	0	—	—

DOA's with any existing high-resolution method; hence, signal-COPY algorithms [17] can not be

used even with perfect knowledge of the array manifold.

Due to presence of coherent wavefronts, second-order statistics are not spatially stationary along the array; hence, it is not meaningful to define SINR at an array element. Instead, we compute the SINR at the output of the optimal processor by employing true statistics. The maximum possible  $\text{SINR}_o$  is found from (5.12) to be 12.677 dB. From Table 7.4, we observe that  $\text{CUM}_2$  performs very well under these severe conditions. Performance of  $\text{CUM}_1$  is effected by strong interferers since this processor does not utilize all of the available information. Finally, we observe that MVDR with correct look-direction cancels the desired signal due to coherence. Note that  $\text{CUM}_2$  exhibits less variations than other processors.

To gain more insight into the operation of the processors, we illustrate the beampatterns for MVDR and  $\text{CUM}_2$  in Figure 7.6. We focus on the region where the wavefronts are received by the array. It is observed that the MVDR processor does not null the jammer from  $-1^\circ$ , since it maintains the look-direction constraint for  $0^\circ$  and tries to minimize the output power by destructively combining the coherent wavefronts. On the other hand,  $\text{CUM}_2$  is blind to Gaussian interferers, and, as in Experiment 2, it estimates the *generalized* steering vector of the desired signal and combines the wavefronts to enhance SINR at the output.  $\text{CUM}_2$  puts a null on the jammer from  $-1^\circ$ , destructively combines the wavefronts from the first jammer by weight-phasing rather than

Table 7.4: Results from 100 Monte-Carlo Runs for Experiment 4

Processor	$\text{SINR}_o$ (dB)	
	Mean	Std
MVDR	-28.424	4.405
$\text{CUM}_1$	4.110	2.118
$\text{CUM}_2$	10.290	0.746
$C^2$	11.879	0.627

null-steering, and reinforces the wavefronts from the desired source.

Finally, we implemented the  $C^2$  beamformer suggested in Section 4.2: we first estimated the steering vector as done for  $CUM_2$ , but then further projected it into the subspace spanned by the principal eigenvectors of the sample covariance matrix. We used the resultant vector as the estimate of the desired signal steering vector, and constructed an MVDR beamformer based on it. The performance of the resultant processor is demonstrated in Table 7.4.

We observe that by combining cumulants with covariance information, we obtain the best results.

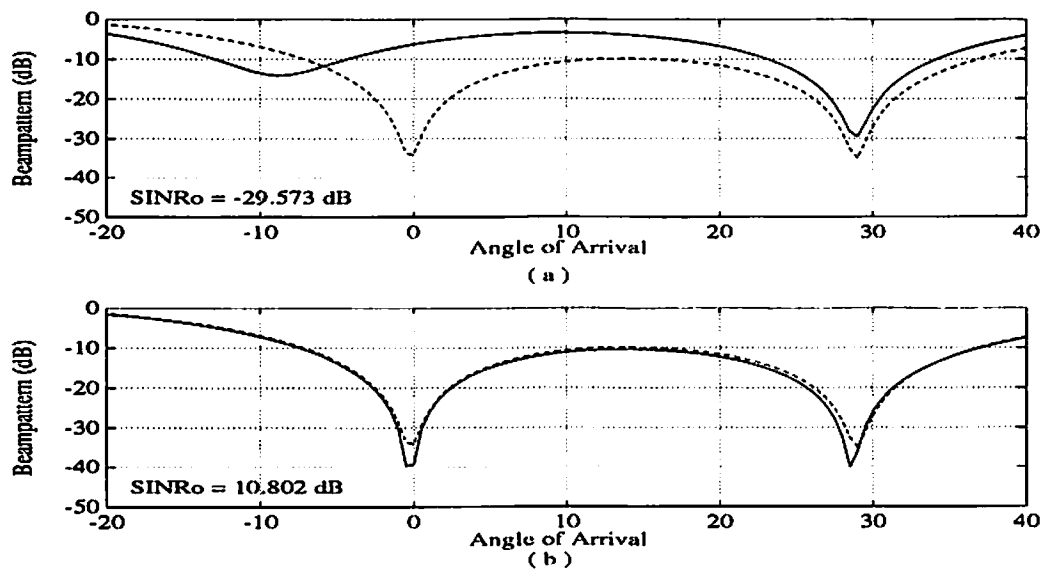


Figure 7.6: Beampatterns and array gains of processors: (a) MVDR with correct look direction, (b)  $CUM_2$ . The optimum pattern is illustrated in dashed lines for comparison purposes.

## 7.5 Experiment 5: Adaptive Processing

In this experiment, we demonstrate the results from the adaptive version of  $CUM_1$  approach as described in Chapter 6. We employed the 10 element uniform linear array of previous experiments.

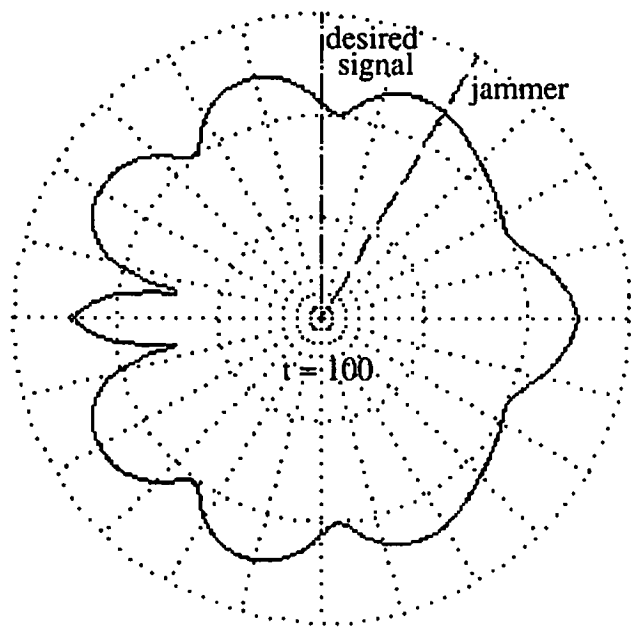
The initial pattern of the beamformer is designed to be isotropic, by letting  $\mathbf{c}(0) = [1, 0, \dots, 0]^T$ . Desired signal illuminates the array from broadside with SNR=10 dB. A jammer with power equal to that of the desired source is present at  $30^\circ$ . Note that there is no nonstationarity involved in this experiment; our aim is to demonstrate the evolution of the beamforming process and indicate the data lengths required for cumulant and covariance estimation. Tracking properties will be included in our future work, including comparisons with adaptive versions of CUM<sub>2</sub> and C<sup>2</sup> processors.

Figure 7.7 illustrates the beampattern of the adaptive CUM<sub>1</sub> processor as time evolves. After 100 snapshots, the beampattern is still close to isotropic. At 300 snapshots, covariance matrix estimate is improved, indicating the presence of desired signal from broadside. At this time point, the cumulant-based steering vector estimate has not matured, so it can not prevent the desired signal from being cancelled. After 500 snapshots, cumulant estimates get better, and there is a tendency to cancel the interference rather than the desired signal. Finally, after 700 snapshots the processor removes the interference by null steering.

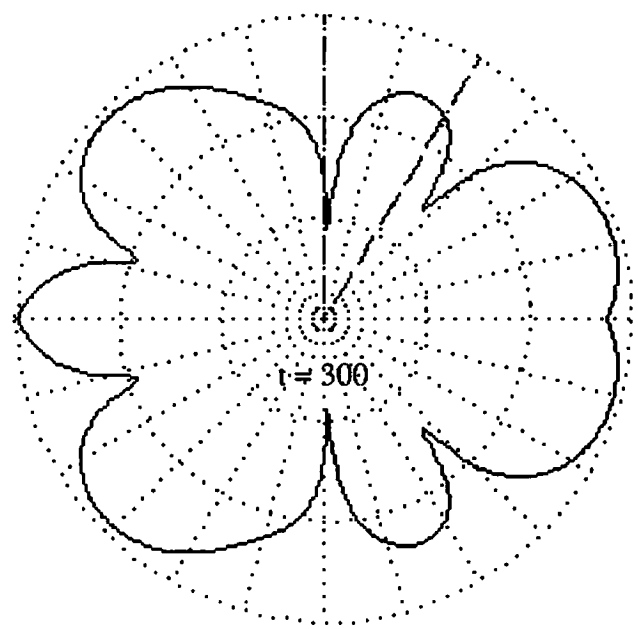
## 7.6 Experiment 6: Effects of Data Length

In this experiment, we employ the linear array of Experiment 1, with the same noise conditions, and vary the data length to observe the behavior of the beamformers CUM<sub>1</sub>, CUM<sub>2</sub>, MVDR<sub>1</sub> and MVDR<sub>2</sub>. Figure 7.8 demonstrates the variation of white-noise gain of the processors with data length, for 0 dB and 20 dB SNR levels. Each point on the plots is obtained by averaging the results from 50 Monte-Carlo simulations.

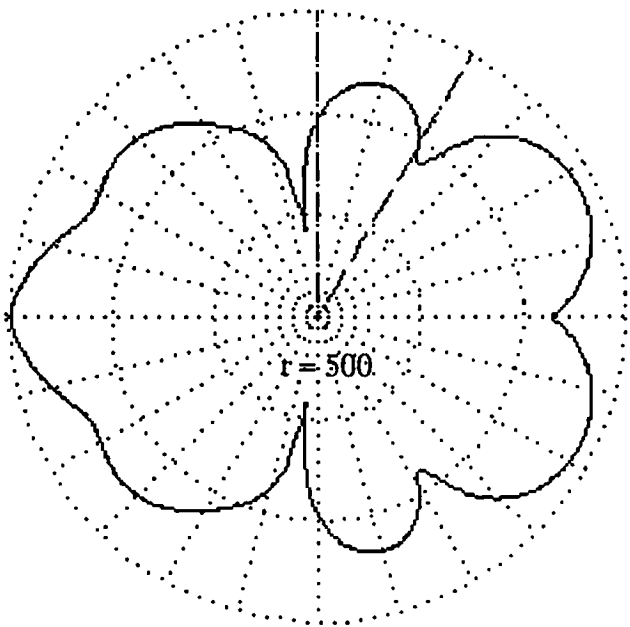
From Figure 7.8a it is clear that CUM<sub>2</sub> outperforms all the processors, including MVDR<sub>2</sub> which utilizes the correct look direction for all data lengths. Furthermore, small sample properties



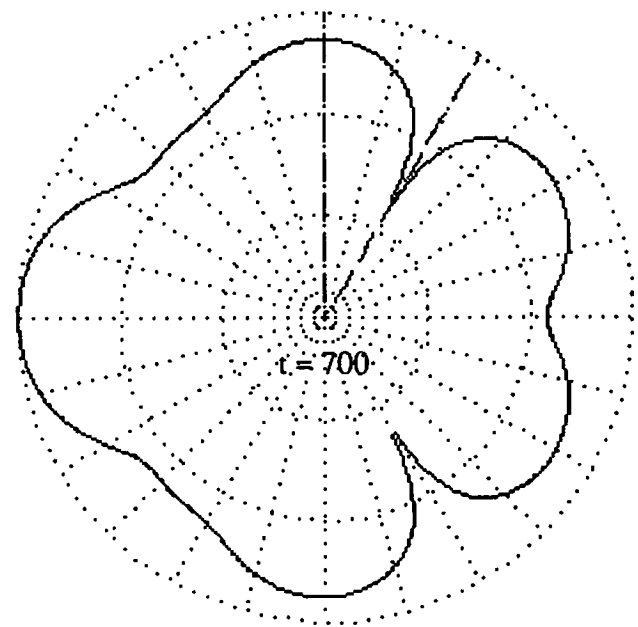
(a)



(b)



(c)



(d)

Figure 7.7: Beampattern of the adaptive CUM<sub>1</sub> processor as a function of time: desired signal is from broadside and the jammer is from  $30^\circ$  as indicated. (a)  $t=100$ , (b)  $t=300$ , (c)  $t=500$ , (d)  $t=700$ .

of  $CUM_2$  are quite impressive, motivating further research for developing its adaptive version. Low SNR masks the mismatch in  $MVDR_2$  due to the use of sample covariance matrix; hence, as can be seen from Figure 7.8a,  $CUM_1$  is inferior to  $MVDR_2$ .

Figures 7.8b and 7.8c, indicate the effect of higher SNR on performance.  $CUM_1$  and  $CUM_2$  perform almost identical for all data lengths. Their gain is larger than 9 dB even for less than 50 snapshots.  $MVDR_2$  can not recover in this experiment since the mismatch results in severe signal cancellation. We do not include the response of  $MVDR_1$ , because its performance drifts around -35 dB.

These results indicate that our approach has very *promising small sample behavior that deserves more research*. This will be a topic of another report.

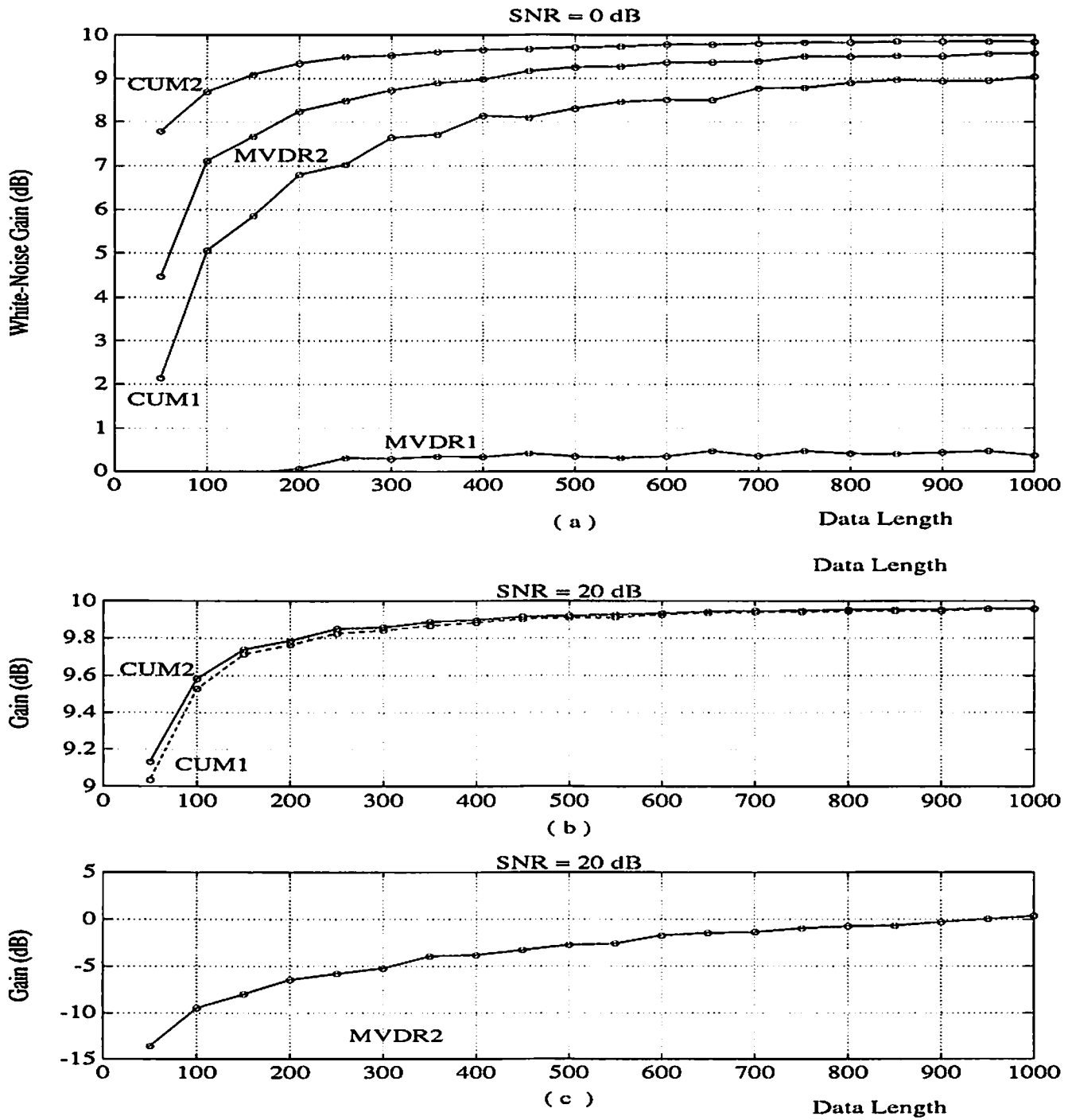


Figure 7.8: Performance of processors with varying data length: (a) SNR=0 dB, (b) SNR=20 dB, CUM<sub>1</sub> and CUM<sub>2</sub>, (c) SNR=20 dB, MVDR<sub>2</sub>.

## Chapter 8

# Conclusions

We have presented optimum beamforming algorithms for non-Gaussian signals, which are based on fourth-order cumulants of the data received by the array. Our proposed methods do not make any assumption about the sensor locations and characteristics, i.e., they are blind beamforming methods. Cumulant-based estimation is employed to identify the steering vector of the signal of interest and MVDR beamforming using this estimate is used to remove Gaussian interference components. We have suggested several approaches to combat effects of estimation errors. We have also implemented a recursive version of the method to enable real-time beamforming. Simulation experiments demonstrate the performance of our approaches in a wide variety of situations. It is important to emphasize that the proposed methods outperform the MVDR beamformer that uses exactly known look-direction information.

In our future work, we shall address the problem of optimum beamforming in the presence of multiple non-Gaussian interferers and design of adaptive algorithms with better convergence properties.



## Appendix A

# Third-order statistics based estimation

In this appendix, we develop a method to estimate the steering vector of the desired non-Gaussian signal, based on third-order statistics. Unlike communication signals, speech and sonar signals, consisting of phase-coupled sinusoids, possess non-zero third-order cumulants. In addition, the estimates of third-order statistics exhibit less variance than that of fourth-order cumulants. Therefore, it is important to present a beamforming procedure based on third-order statistics.

Let us assume the presence of a zero-mean, non-Gaussian desired signal,  $d(t)$ , with a non-zero zero-lag third-order cumulant,  $\gamma_{d,3} = E \{d(t) d^H(t) d(t)\}$ , that is corrupted by undesired signals whose third-order cumulants are zero. Note that the restriction on the interference characteristics is relaxed; i.e., we only require the third-order cumulants of the undesired signals be zero, rather than assuming Gaussian interferers. Consider the vector  $\mathbf{c}$ , formed as

$$\mathbf{c}_l = \text{cum}\{r_{i_1}(t), r_{i_2}^H(t), r_l(t)\} \quad (\text{A.1})$$

Then, using the signal model (5.4) and [CP1], we obtain

$$c_l = b_{i_1} b_{i_2}^H \gamma_{d,3} \quad b_l \quad 1 \leq i_1, i_2 \leq M \quad (\text{A.2})$$

or, in vector form

$$\mathbf{c} = (b_{i_1} b_{i_2}^H \gamma_{d,3}) \mathbf{b} \quad (\text{A.3})$$

Equation (A.3) is the “third-order” counterpart to (5.5) and its generalized version (B.3).

## Appendix B

# Full utilization of array data

In this appendix, we extend the estimation procedure suggested in Section 4.1 to fully utilize the array data. The estimation procedures presented previously in this report are in fact special cases of the estimation procedure that will be presented here. Consider the vector  $\mathbf{c}$  formed as

$$c_l = \text{cum}\{r_{i_1}(t), r_{i_2}^H(t), r_{i_3}^H(t), r_l(t)\} \quad l = 1, 2, \dots, M \text{ and } 1 \leq i_1, i_2, i_3 \leq M. \quad (\text{B.1})$$

Using the signal model (5.4) and [CP1], we obtain

$$c_l = b_{i_1} b_{i_2}^H b_{i_3}^H \gamma_{d,A} b_l \quad (\text{B.2})$$

or in vector form,

$$\mathbf{c} = (b_{i_1} b_{i_2}^H b_{i_3}^H \gamma_{d,A}) \mathbf{b} \quad (\text{B.3})$$

implying that the vector  $\mathbf{c}$  is identical to the desired signal steering vector up to a scale factor.

The algorithm of Section 4.1 lets  $i_1 = i_2 = i_3 = i$ , and varies  $i$  in the range  $1 \leq i \leq M$ , to

obtain a rank one  $M \times M$  matrix, from which the estimation procedure is completed by identifying the left eigenvector with the largest singular value. On the other hand, from (B.2) we realize that we can collect more vectors by varying  $i_1, i_2, i_3$  individually. However, there is a redundancy arising from the definition of fourth-order cumulants: the maximal set of non-redundant cumulants,  $cum\{r_{i_1}(t), r_{i_2}^H(t), r_{i_3}^H(t), r_{i_4}(t)\}$ , is obtained for the following range of indexes,  $\{1 \leq i_1 \leq M, 1 \leq i_4 \leq i_1, 1 \leq i_2 \leq i_1, 1 \leq i_3 \leq i_2\}$ . Performing an SVD on the matrix by stacking non-redundant estimated steering vectors, we completely utilize the array data. This approach, however, requires an SVD analysis of a large matrix, which may turn out to be prohibitive for real-time applications.

# Bibliography

- [1] R.A. Monzingo and T.W. Miller, *Introduction to Adaptive Arrays*. John-Wiley & Sons, Inc., 1980.
- [2] S. Haykin, ed., *Array Processing: Applications to Radar*. Dowden, Hutchinson & Ross, Inc., 1980.
- [3] S. Haykin, ed., *Array Signal Processing*. Prentice-Hall, New-Jersey, 1984.
- [4] Special Issue on Adaptive Antenna Systems, *IEEE Antennas Propagat.*, vol.AP-34, March 1986.
- [5] J. Marr, "A selected bibliography on adaptive antenna arrays," *IEEE Trans. Aerosp. Electron. Syst.*, AES-22, no.6, pp.781-798, November 1986.
- [6] B. Van Veen and K. Buckley. "Beamforming: a versatile approach to spatial filtering," *IEEE ASSP Magazine*, pp.4-24, April 1988.
- [7] R.T. Compton, *Adaptive Antennas: Concepts and Performance*. Prentice-Hall, New-Jersey, 1988.
- [8] S.U. Pillai, *Array Signal Processing*. Springer-Verlag, New-York, 1989.

- [9] S. Haykin, ed., *Advances in Spectrum Estimation and Array Processing*. Prentice-Hall, New-Jersey, 1991.
- [10] J. Capon, "High-resolution frequency-wavenumber spectral analysis," *Proc. of IEEE*, vol.57, no.8, pp.1408–1418, August 1969.
- [11] W. Gabriel, "Spectral analysis and adaptive array superresolution techniques," *Proc. IEEE*, vol.68, no.6, pp.654–666, June 1980.
- [12] D. Johnson and S. DeGraaf, "Improving the resolution of bearing in passive sonar arrays by eigenvalue analysis," *IEEE Trans. Acoust., Speech, Signal Processing*, vol.ASSP-30, no.4, pp.638–647, August 1982.
- [13] R. Kumaresan and D. Tufts, "Estimating the angles of arrival of multiple plane waves," *IEEE Trans. Aerospace and Electronic Systems*, vol.AES-19, no.1, pp.134–139, January 1983.
- [14] G. Bienvenu and L. Kopp, "Optimality of high resolution array processing using the eigensystem approach," *IEEE Trans. Acoust., Speech, Signal Processing*, vol.ASSP-31, no.5, pp.1235–1247, October 1983.
- [15] S. DeGraaf and D. Johnson. "Capability of array processing algorithms to estimate source bearings," *IEEE Trans. Acoust., Speech, Signal Processing*, vol.ASSP-33, no.6, pp.1368–1379, December 1985.
- [16] W. Gabriel, "Using spectral estimation techniques in adaptive processing antenna systems," *IEEE Trans. Antennas and Propagation*, vol.AP-34, no.4, pp.291–300, March 1986.
- [17] R.O. Schmidt, "Multiple emitter location and signal parameter estimation," *IEEE Trans. Antennas and Propagation*, vol.AP-34, no.3, pp.276–280, March 1986.

- [18] R.O. Schmidt and R.E. Franks, "Multiple source DF signal processing: an experimental system," *IEEE Trans. Antennas and Propagation*, vol.AP-34, no.3, pp.281-290, March 1986.
- [19] A.J. Weiss, A.S. Willsky and B.C. Levy, "Eigenstructure approach for array processing with unknown intensity coefficients," *IEEE Trans. Acoust., Speech, Signal Processing*, vol.ASSP-36, no.10, pp.1613-1617, October 1988.
- [20] R. Roy and T. Kailath, "ESPRIT—Estimation of signal parameters via rotational invariance techniques," *IEEE Trans. Acoust., Speech, Signal Processing*, vol.ASSP-37, no.7, pp.984-995, July 1989.
- [21] M. Viberg and B. Ottersten, "Sensor array processing based on subspace fitting," *IEEE Trans. Acoust., Speech, Signal Processing*, vol.ASSP-39, no.5, pp.1110-1121, May 1991.
- [22] Y. Rockah and P.M. Schultheiss, "Array shape calibration using sources in unknown locations—part I: far-field sources," *IEEE Trans. Acoust., Speech, Signal Processing*, vol.ASSP-35, no.3, pp.286-299, March 1987.
- [23] A.J. Weiss and B. Friedlander, "Array shape calibration using sources in unknown locations—a maximum-likelihood approach," *IEEE Trans. Acoust., Speech, Signal Processing*, vol.ASSP-37, no.12, pp.1958-1966, December 1989.
- [24] C.L. Zahm, "Effects of errors in the direction of incidence on the performance of an adaptive array," *Proc. IEEE*, vol.60, pp.1008-1009, August 1972.
- [25] H. Cox, "Resolving power and sensitivity to mismatch of optimum array processors." *J. of Acoust. Soc. Amer.*, vol.54, no.3, pp.771-785, 1973.

- [26] A.M. Vural, "Effects of perturbations on the performance of optimum/adaptive arrays," *IEEE Trans. Aerosp. Electron. Syst.*, vol.AES-15, pp.76-87, January 1979.
- [27] R.T. Compton, "Pointing accuracy and dynamic range in a steered beam adaptive array," *IEEE Trans. Aerosp. Electron. Syst.*, vol.AES-16, pp.280-287, May 1980.
- [28] R.T. Compton, "The effect of random steering error vectors in the Applebaum adaptive array," *IEEE Trans. Aerosp. Electron. Syst.*, vol.AES-18, pp.392-400, September 1982.
- [29] L.C. Godara, "Error analysis of optimal antenna array processors," *IEEE Trans. Aerosp. Electron. Syst.*, vol.AES-22, July 1986.
- [30] H. Cox, H.M. Zeskind and M.M. Owen, "Effects of amplitude and phase errors on linear predictive array processors," *IEEE Trans. Acoust., Speech, Signal Processing*, vol.ASSP-36, no.1, January 1988.
- [31] B. Friedlander and B. Porat, "Performance analysis of a null-steering algorithm based on direction-of-arrival estimation," *IEEE Trans. Acoust., Speech, Signal Processing*, vol.ASSP-37, no.4, pp.461-466, April 1989.
- [32] B. Friedlander, "A sensitivity analysis of the MUSIC algorithm," *IEEE Trans. Acoust., Speech, Signal Processing*, vol.ASSP-38, no.10, pp.1740-1751, October 1990.
- [33] D. Feldman and L.J. Griffiths, "A constraint projection approach for robust adaptive beamforming," in *Proc. IEEE Intl. Conf. Acoust., Speech, Signal Processing*, pp.1381-1384, May 1991.
- [34] C.L. Zahm, "Application of adaptive arrays to suppress strong jammers in the presence of weak signals," *IEEE Trans. Aerosp. Electron. Syst.*, vol. AES-9, pp.260-271, 1973.



- [35] H. Cox, H.M. Zeskind and M.M. Owen, "Robust adaptive beamforming," *IEEE Trans. Acoust., Speech, Signal Processing*, vol.ASSP-35, no.10, pp.1365-1376, October 1987.
- [36] R.A. Scholtz, "How do you define bandwidth," *Proceedings of the International Telemetry Conference*, Los Angeles, California, pp.281-288, October 1972.
- [37] D. Slepian, "On bandwidth," *Proc. of IEEE*, vol.64, pp. 292-300, 1976.
- [38] B. Friedlander, "A signal subspace method for adaptive interference cancellation," *IEEE Trans. Acoust., Speech, Signal Processing*, vol.ASSP-36, no.12, pp.1835-1845, December 1988.
- [39] A. Paulraj and T. Kailath, "Eigenstructure methods for direction of arrival estimation in the presence of unknown noise fields," *IEEE Trans. Acoust., Speech, Signal Processing*, vol.ASSP-34, no.1, pp.13-20, February 1986.
- [40] S. Prasad, R.T. Williams, A.K. Mahalanabis and L.H. Sibul, "A transform-based covariance differencing approach for some classes of parameter estimation problems," *IEEE Trans. Acoust., Speech, Signal Processing*, vol.ASSP-36, no.5, pp.631-641, May 1988.
- [41] P. Ruiz and J.L. Lacoume, "Extraction of independent sources from correlated sources: a solution based on cumulants," *Proc. Vail Workshop on Higher-Order Spectral Analysis*, pp.146-151, June 1989.
- [42] J.F. Cardoso, "Blind identification of independent components with higher-order statistics," *Proc. Vail Workshop on Higher-Order Spectral Analysis*, pp.157-162, June 1989.
- [43] P. Comon, "Separation of stochastic processes," *Proc. Vail Workshop on Higher-Order Spectral Analysis*, pp.174-179, June 1989.

- [44] B. Widrow, K.M. Duvall, R.P. Gooch and W.C. Newman, "Signal cancellation phenomena in adaptive antennas: causes and cures," *IEEE Trans. Antennas and Propagation*, vol.AP-30, no.3, pp.469-478, May 1982.
- [45] T. Shan and T. Kailath, "Adaptive beamforming for coherent signals and interference," *IEEE Trans. Acoust., Speech, Signal Processing*, vol.ASSP-33, no.3, pp.527-536, June 1985.
- [46] T. Shan, M. Wax and T. Kailath, "On spatial smoothing for direction-of-arrival estimation of coherent signals," *IEEE Trans. Acoust., Speech, Signal Processing*, vol.ASSP-33, no.4, pp.806-811, August 1985.
- [47] Y. Su, T. Shan and B. Widrow. " Parallel spatial processing: a cure for signal cancellation in adaptive arrays," *IEEE Trans. Antennas and Propagation*, vol.AP-34, no.3, pp.347-355, March 1986.
- [48] S. Pei, C.C. Yeh and S.C. Chiu, "Modified spatial smoothing for coherent jammer suppression without signal cancellation," *IEEE Trans. Acoust., Speech, Signal Processing*, vol.ASSP-36, no.3, pp.412-414, March 1988.
- [49] R. Williams, S. Prasad, A.K. Mahalanabis and L.H. Sibul, "An improved spatial smoothing technique for bearing estimation in a multipath environment," *IEEE Trans. Acoust., Speech, Signal Processing*, vol.ASSP-36, no.4, pp.425-432, April 1988.
- [50] U. Pillai and B. Kwon. " Forward/backward spatial smoothing schemes for coherent signal identification," *IEEE Trans. Acoust., Speech, Signal Processing*, vol.ASSP-37, no.1, pp.8-15, January 1989.

- [51] V. Reddy, A. Paulraj and T. Kailath, "Performance analysis of the optimum beamformer in the presence of correlated sources and its behavior under spatial smoothing," *IEEE Trans. Acoust., Speech, Signal Processing*, vol.ASSP-35, no.7, pp.927-936, July 1987.
- [52] M. Zoltowski, "On the performance analysis of the MVDR beamformer in the presence of correlated interference," *IEEE Trans. Acoust., Speech, Signal Processing*, vol.ASSP-36, no.6, pp.945-947, June 1988.
- [53] Y. Bresler, V.U. Reddy and T. Kailath, "Optimum beamforming for coherent signal and interferences," *IEEE Trans. Acoust., Speech, Signal Processing*, vol.ASSP-36, no.6, pp.833-843, June 1988.
- [54] C.L. Nikias and M.R. Raghuveer, "Bispectrum estimation: a digital signal processing framework," *Proc. IEEE*, vol.75, no.7, pp.869-891, July 1987.
- [55] J.M. Mendel, "Tutorial on higher-order statistics (spectra) in signal processing and system theory: theoretical results and some applications," in *Proc. IEEE*, vol.79, no.3, pp.278-305, March 1991.
- [56] G.B. Giannakis and M. Tsatsanis, "HOS or SOS for parametric modelling," *Proc. IEEE Intl. Conf. on Acoust., Speech, Signal Processing*, vol.5, pp.3097-3100, May 1991.
- [57] K.S. Lii and M. Rosenblatt. "Deconvolution and estimation of transfer function phase and coefficients for non-Gaussian linear processes," *Ann. Statist.*, vol.10, pp.1195-1208, 1982.
- [58] D.R. Brillinger and M. Rosenblatt, "Asymptotic theory of estimates of  $k$ th-order spectra," in *Spectral Analysis of Time Series*, B. Harris, ed., New-York: John Wiley & Sons, pp.189-232, 1967.

- [59] B. Porat and B. Friedlander, "Direction finding algorithms based on high-order statistics," *IEEE Trans. Acoust., Speech, Signal Processing*, vol. ASSP-39, no. 9, pp. 2016–2024, September 1991.
- [60] T.J. Abatzoglou, J.M. Mendel and G.A. Harada, "The constrained total least squares technique and its applications to harmonic superresolution," *IEEE Trans. Signal Processing*, vol. 39, no. 5, pp. 1070–1087, May 1991.
- [61] D.G. Brennan, "On the maximum signal-to-noise ratio realizable from several noisy signals," *Proc. IRE*, vol. 43, pg. 1350, 1955.
- [62] J.M. Ortega, *Matrix Theory: a second course*. Plenum Press, New-York, 1987.
- [63] R.J. Talham, "Noise correlation functions for unisotropic noise fields," *J. Acoust. Soc. Amer.*, vol. 69, pp. 213–215, January 1981.